Diversity and Effects of Fungicides on the Pecan Phyllosphere Microbiome, and Fungal Interactions with a Novel Yeast

by

Beatrice Mattie Severance

A thesis submitted to the Graduate Faculty of
Auburn University
in partial fulfillment of the
requirements for the Degree of
Master of Science

Auburn, Alabama
August 3, 2024

Keywords: phyllosphere, microbiome, yeast, fungicides

Approved by

Zachary Noel, Chair, Assistant Professor, Plant Pathology
Neha Potnis, Endowed Associate Professor, Plant Pathology
Mark R. Liles, Professor, Biological Sciences

Abstract

The phyllosphere microbiome is one of the largest habitats on earth, hosting any organism that can adapt to it. Phyllosphere yeasts in particular can dominate this habitat, but to this date have been chronically understudied with much novelty left to discover and classify. In the presence of fungicides, phyllosphere yeast taxa have been shown to have altered abundance. Pecans are native to the southeastern US, and are grown for nutrients like fiber, copper, and zinc. Fungal pathogens like powdery mildew and scab can affect the fitness of nuts. These pathogens are controlled by fungicide applications, up to and over 10 times a growing season. Under these high fungicide usage conditions, it is hypothesized that these chemical applications may alter phyllosphere yeast taxa abundance. Chapter 1 reviews previous literature discussing phyllosphere microbiomes and effects of fungicides on natural community members, as well as current knowledge of phyllosphere yeasts. In chapter 2, we seek to classify the pecan phyllosphere microbiome from a two-year experiment using molecular and bioinformatic tools for community profiling and analysis. We hypothesize that fungicide applications will have a non-targeted effect on the phyllosphere microbiome, specifically regarding yeast species. We also predict that fungicide-treated leaves will have a disrupted network structure compared to non-treated control leaves. Thus, 12 pecan trees were sampled before and after fungicide applications over the course of two years, 2021 and 2022, to provide community profiling and determine effects of fungicides on community members. Findings from this study support the hypothesis that fungicides have a non-targeted effect on the pecan phyllosphere microbiome, decreasing richness of fungicide-treated leaves and causing a significant difference in

community composition in 2021. In addition, findings show that network hubs change between non-treated leaves and treated leaves. In chapter 3, we explore fungal-fungal interactions between a selection of environmental yeast species and a group of fungi to support the hypothesis that these environmental isolates can produce compounds that inhibit fungi. After this, we hone in on a novel Dothideomycete yeast, EMM_F3, to explore metabolic properties that may be causing inhibition of fungi—specifically *Fusarium graminearum* PH-1—, and taxonomically place it using comparative genomics techniques to other high quality Dothideomycete species. Initial findings support the hypothesis that environmental yeasts can have an inhibitory effect on various fungi. When focusing on EMM_F3, we determined that inhibition to PH-1 was due to metabolites, and we attempted to classify these metabolites through both genome sequencing and gas chromatography-mass spectrometry. Metabolites of interest included clavaric acid, tridecane, and nonadecane. Genome comparison placed EMM_F3 closely to relatives *Delphinella strobiligena* (a pine pathogen), and *Aureobasidium pullulans* (an extremophile yeast that has known biocontrol properties). In Chapter 4 we discuss the impacts of these experiments. Thus, this thesis promotes ideas for balancing pest management and preservation of biodiversity in agricultural systems and encourages exploration of the phyllosphere—specifically yeast species—to help understand species diversity and microbial interactions, as well as elucidate new biocontrol directions or new biologically useful metabolites or proteins.

Acknowledgements

I want to thank my advisor, Dr. Zachary Noel, for his stellar mentorship throughout my time at Auburn. I am thankful to my committee members, Dr. Neha Potnis and Dr. Mark Liles, for their guidance and contributions to my research that I would have missed independently. I would also like to thank Jason Burkett at the Plant Breeding Unit of the E.V. Smith station for helping coordinate fungicide applications on our pecan orchard throughout our experiment. In addition, I would like to thank Melissa Boersma from the Auburn University Department of Chemistry for her assistance with mass spectrometry. I am grateful for the organizations that funded my research, including the Auburn University Department of Entomology and Plant Pathology, Auburn University College of Agriculture AgrSEED program, BASF, the Alabama Soybean Commission, the USDA National Institute of Food and Agriculture, Hatch Project 1025628, and USDA National Institute of Food and Agriculture, Agriculture and Food Research Initiative award number 2023-67014-39903. I also have eternal gratitude for Oluwakemisola Olofintila, Laura Rodriguez, Dr. Morgan Bragg, Logan Luchs, Bibek Dabargainya, and Sachida Pokhrel for offering their assistance and motivating me when I needed it most. I am grateful to the Auburn University Miller Writing Center, and particularly Huan Liu, for providing me with regular editing opportunities for my thesis writing.

I am grateful to my family, Tara Severance, Ben Severance, and Josey Severance, for their never-ending love and support throughout my graduate journey. I want to thank my partner, Joseph Gerard, for being somebody I can count on to be there for me when I need a shoulder to lean on, as well as a person with whom I can enjoy life. Last but not least, I would like to thank

the Graduate Student Council and my fellow colleagues in the departments of entomology and plant pathology for giving me a strong sense of community at a time when I'm learning how to become a self-sufficient adult.

Table of Contents

List of Tables

List of Figures

1. CHAPTER ONE

Introduction and Literature Review

Pecan Scab

Pecans (*Carya illinoinensis*) are a prized agricultural crop and native to the United States, generating a total of $399 million in 2020 (NASS). The phenolic compounds from their shells have even been shown to provide antitumor activity (Hilbig et al., 2018). However, as with most commercial crops, pecan trees are not immune to the presence of pathogens. Pecan scab is the most prevalent disease of pecan, and scab infection can significantly affect yield, as it is the number one most devastating pecan disease in the southeastern United States (Demaree, 1924). Pecan scab is caused by a fungus called *Venturia effusa*, primarily known by the anamorphic name *Fusicladium effusum* (Winter et al., 2022).

V. effusa falls under the phylum Ascomycota, class Dothideomycetes (Winter et al., 2022). In a study by Bock et al. (2014), recombination rates were analyzed and determined to be similar to organisms that showed signs of a sexual stage but had not been proven, even though other factors of recombination rates did not add up. Though primarily known as an asexual fungus, Charlton et al. (2019) first described the presence of a sexual stage in *V. effusa*. This study confirmed the existence of a sexual stage in *V. effusa*, with an extremely long experimental stage of up to four months to produce asci in all treatment groups. The knowledge generated by this study was immense and currently helps aid future research since *V. effusa* appears to be similar to apple scab (*Venturia inequalis*) in function. Current challenges in studying the epidemiology of pecan scab are related to a limited understanding of survival structures and habitats in leaf litter and multiple morphologically similar organisms like *Mycosphaerella*.

Pecan scab causes disease by proliferating on young leaves before blooming, and spreading to the nuts as growth continues (Brock, 2016). When the nuts begin to harden, scab has already dealt much damage. Commercial facilities will use fungicides over ten times a season to control the detrimental effects of scab to have quality nuts at harvest (Ellis, 2000). However, cultivars can affect commercial fungicide applications since cultivars with low susceptibility, like Elliot or Lakota, may be sprayed only three times with little to no scab presence, while high susceptibility cultivars, like Desirable or Pawnee, require at least eight to achieve the same effect. Conner (2002) studied the effects of different races of *V. effusa* on pecan trees and found that the pathogen was more likely to colonize the cultivar from which they were initially isolated, which may be useful in informing growers on which races to incorporate into their commercial practice.

The selection of cultivars with scab tolerance may aid commercial growers economically due to the lower number of fungicide applications. However, certain nut qualities of susceptible cultivars like flavor and size are desired by consumers, where extra fungicide applications are necessary. In addition, utilizing tolerant cultivars will enable pathogens to overcome plant defenses and cause breakthrough infection, which may only increase reliance on fungicide applications. This has been shown with *Venturia inequalis* in apples (Beckerman et al., 2013). Transitioning cultivars to low-susceptibility varieties is also problematic because it takes more than 10 years for pecan trees to reach maturity. Therefore, regular fungicide applications are still widely used and necessary for pecan production.

Fungicide Application

Combined chemical and application cost for pecan can range from $25 to $40 per acre (Nesbitt, 2013). Chemical control of *V. effusa* involves both broad- and narrow-spectrum

fungicides. Broad-spectrum fungicides aim to control general fungal infection in plants and generally do not have a specific target species or mechanism, while narrow-spectrum fungicides aim to target specific pathogens and may differ depending on the pathogen targeted. The fungicides Phostrol®, Stratego®, SUPER TIN 4L, Absolute® Maxx, Elast, and Miravis® Top are commonly sprayed on pecan orchards. Phostrol® contains phosphorous acid salts, which target phosphonates and is a Group 7 fungicide (FRAC). It is frequently sprayed at a rate of 40 fl oz/acre^{-1} and has a broad-spectrum control of the pathogens that cause downy mildew and pecan scab (Nufarm, 2020). Stratego ® is a fungicide that contains the active ingredients trifloxystrobin and propiconazole (Bayer 2023), which target complex III of fungal respiration and C14-demethylation in sterol biosynthesis, respectively (FRAC). Stratego ® YLD is applied at a rate of 10 fl oz acre^{-1}. SUPER TIN 4L is a fungicide that contains the active ingredient triphenyltin hydroxide, which controls for powdery mildew and scab in pecan, and is applied to a pecan orchard at the recommended rate of 12 fl oz acre^{-1} (United Phosphorous, Inc., 2009). Triphenyltin hydroxide is a Class 30 fungicide (Nesbitt, 2013).

The fungicide Absolute® Maxx is applied to a pecan orchard at a rate of 7.67 fl oz acre^{-1}. Absolute® Maxx contains the active ingredients tebuconazole and trifloxystrobin, groups similar to Stratego ®. Tebuconazole targets C14-demethylase in sterol biosynthesis, and trifloxystrobin is a quinone outside inhibitor (FRAC, 2024). Elast is a fungicide that contains the active ingredient dodine, which has the proposed mode of action of cell membrane disruption and is in Group U12 (FRAC, 2024); this is commonly applied at a rate of 25 fl oz acre^{-1}. It is also commonly sprayed with SUPER TIN in pecan applications (Wells, 2021). Finally, Miravis® Top (Syngenta, 2019) is a fungicide that contains the active ingredients pydiflumentofen—a succinate dehydrogenase inhibitor—and difenoconazole—a triazole demethylation inhibitor—, which are

in FRAC groups 7 and 3, respectively (FRAC, 2024). Miravis® Top is commonly applied at a rate of 13.6 fl oz $acre^{-1}$. While narrow-spectrum fungicides are more targeted, they may still be causing off-target effects on non-pathogenic members of the community. Pecan trees are heavily pressured by fungicide use; thus, members may be more resilient than communities that do not undergo this amount of stress.

Depending on cultivar, pecan orchards can be sprayed an average of three times for resistant cultivars, seven for a cultivar in the mid-range, and ten or more for susceptible cultivars (Wells, 2021). Wells and other University of Georgia extension community members recommend sprays to begin mid-late April and continue into August, depending on susceptibility. Due to the pressure of pecan scab, commercial practice demands the application of broad-spectrum fungicides. This provides sufficient control of scab and introduces curiosity on how the native microbiome handles this pressure.

Disturbance Ecology

With the potential for commercial fungicides to cause non-target effects, knowledge of disturbance ecology becomes useful. Early definitions of disturbance ecology can be attributed to Bender et al. from a 1984 publication. In this manuscript, perturbations could be either 1) pulsed or a short-term sudden change in a community that recovers after, or 2) press, a continuous disturbance that causes permanent damage. Modern-day terminology has been well-defined by Ashley Shade. In the presence of a disturbance (natural disaster, fungicide application, etc.), one of four scenarios can occur: resistance, resilience, redundancy, and regime shift (Shade, 2023). Resistance involves maintaining the structure and function of the microbial community, resilience involves structure and function that both recover, redundancy recovers function but retains an altered structure, and regime shift involves a permanently altered function. These

terms echo the original definitions in 1984 but add more clarity in areas where scientists may have needed clarification (Glasby et al., 1996).

Chapter 2 of my thesis will discuss disturbance ecology, specifically fungicides and the effects they can cause on the phyllosphere of pecans. Fungal microbiome diversity has been studied previously, though many studies have been performed on the rhizosphere microbiome. Huet et al. (2023) showed that soil community depletion (a disturbance) caused remaining microbial communities to increase relative fitness and abundance and could significantly alter soil pH. The phyllosphere microbiome is of heightened interest in my thesis because aerial fungicide applications can directly affect the communities that live on or in leaves – the battleground for fungal plant pathogens like *V. effusa*. Studies like this have been performed in the past, though there is more information on bacteria. For example, a study by Chen (2021) studied the effects of pesticides on bacterial communities. It concluded that non-target bacterial communities can be significantly affected, with potentially beneficial bacteria like *Flavobacterium* and *Sphingomonas* among the most sensitive responders. The decline in beneficial populations can cause a regime shift or a loss of diversity. In addition, pesticide exposure causes heightened tolerance in potentially pathogenic species and high resilience in treatments where a broad-spectrum pesticide was used (Chen et al., 2021).

For disturbances to the fungal community, fungicides applied to wheat were shown to alter the relative abundance of many saprotrophs, while the targeted pathogens remained mixed in terms of presence (Karlsson et al., 2014). This implies that while fungicides contain pathogen presence to an extent, this may be insignificant, and other community members may be lost. Another study showed an increase in *Fusarium* sp. after fungicide applications, which contradicts the purpose of fungicides (find this source in the Knorr paper).

Relevant to disturbance ecology, multiple studies have shown that while some fungal taxa are negatively affected by applying broad or narrow-spectrum fungicides, the presence of yeast taxa remains stable or even increases. Dickinson et al. (1976) studied the impacts of fungicides on a wheat system. They observed that yeast populations drastically increased throughout the season, likely due to fungicides preventing the proliferation of other populations. Similarly, a study by Gdanetz et al. (2021) observed effects of management practice on multiple crops and found that yeasts remain prevalent throughout the season despite any disturbances. In addition, another study done in wheat observed that the core taxa of the microbiome included six basidiomycete yeasts, and after fungicide application *Sporobolomyces* and *Cryptococcus* increased in abundance (Knorr et al., 2019). The conclusion of this study suggested that this was because the yeasts exploit available space from dead microbes, implying a saprobic nature.

In addition, previous research has studied microbiome recovery after fungicide application to corn and soybean (Noel et al., 2022). Noel and collaborators noticed significant non-target effects on beneficial yeast taxa and that these yeast taxa co-occurred with beneficial plant growth-promoting bacteria. This was from a single fungicide application, and pecan endures much harsher disturbances, indicating that beneficial microbiome members will be severely affected by this. Phyllosphere yeasts are of specific importance because they aid in pathogen suppression (Freimoser, 2019), alter nectar to attract pollinators (Cadez, 2010, Shaeffer, 2017), build a hearty microbiome structure (Agler, 2016), and produce phytohormones (Sun, 2014). The possibilities of phyllosphere yeast are numerous, yet little is known about these species. Elucidating a particular novel yeast will be the focus of Chapter 3.

Many studies on microbiome and disturbance ecology study annual crop systems, which leaves room for further research. Blueberries are a perennial crop in which fungicide application

has been studied, and while fungi are affected by fungicides, bacteria are not as strongly affected (Lloyd et al., 2021). This study also concluded that prothioconazole may have a less deleterious effect on potential crop symbionts, which could help determine treatments that do not harm off-target members. Redford et al. (2009) experiment worked on a leaf surface's bacterial succession over a growing season and determined that controlling various environmental factors across temporal space was difficult, if not impossible. They stated that variability between trees on a single date was more similar than a single tree over time. They suggested this was because frequent disturbance events and multiple succession sequences may occur throughout a season. These factors are essential in determining how best to sample a microbiome, and the confounding factors can limit the conclusions made.

Phyllosphere Yeasts

The phyllosphere is the aerial or above-ground plant parts, including leaves, stems, flowers, and fruits (Lindow & Brandl, 2003; Knief et al., 2010). The phyllosphere encompasses almost double the amount of surface area as the total land surface area (Vorholt, 2012), indicative of massive amounts of space for various microorganisms to colonize. Despite this large space, the organisms that colonize these habitats have been historically understudied (Vorholt, 2012).

Phyllosphere yeasts have often been described as abundant globally but have yet to be described in extensive detail (Lindow & Brandl, 2003). Some of these yeasts, like *Aureobasidium pullulans*, have been shown to have biocontrol properties (Zhang et al., 2012) and have biocontrol products on the market (Weiss et al., 2006; Kunz, 2004). Because of this, it is important to study other phyllosphere yeasts in order to uncover and potentially utilize these properties to aid in antifungal discovery, which is in high demand in both agricultural and

medical circumstances. Studying phyllosphere yeasts is also important in order to document natural diversity in habitats that still contain much species novelty.

Conclusions and Thesis Objectives

The literature reviewed suggests that there is more to be studied concerning fungicide application on perennial crops in a high-pressure environment, as well as a knowledge gap on phyllosphere yeast-like fungi. Therefore, this thesis aims to 1) identify the community makeup on pecan leaves and how communities shift over time due to fungicide applications and 2) study novel yeast-like fungi and elucidate critical characteristics of what may be contributing to leaf surfaces worldwide. In Chapter 2, I elucidate the microbiome of the pecan phyllosphere over a two-year sampling period, sampling before fungicide applications and explaining the observed changes. In Chapter 3, I examined phyllosphere yeast interactions on agar medium with fungi representing three fungal lineages and one oomycete. These interactions pointed to one yeast isolate (EMM_F3) that consistently generated inhibition zones against *Fusarium graminearum* PH-1. Interestingly, this yeast was also a novel organism, considering its ITS sequence only matched other known fungi by 87.9%. Therefore, a draft genome was sequenced, and potential metabolites were examined via genomics and gas chromatography-mass spectrometry. Furthermore, the yeast isolate was placed on the fungal tree of life and was compared to other closely related Dothideomycete taxa. Overall, these experiments aim to help promote ideas for balancing pest management and preservation of biodiversity in agricultural systems and encourages exploration of the phyllosphere—specifically yeast species—to help understand species diversity and microbial interactions, as well as elucidate new biocontrol directions or new biologically useful metabolites or proteins.

2. CHAPTER TWO

The effects of fungicides on the pecan phyllosphere fungal diversity

Abstract

Pecan trees (*Carya illinoinensis*) produce nuts that are rich in nutrients like fiber and zinc. Pecan scab (*Venturia effusa*) is a fungal pathogen that causes heavy disease pressure on the crop every season. Scab is controlled by over ten fungicide applications on non-resistant cultivars, which is a significant expense to consider. Despite this, fungicides are necessary to manage disease and thus cause a threat to natural fungal biodiversity. This study aims to explore what other microbes live on a pecan leaf and what species are potentially being affected indirectly by fungicide applications. The research involved sampling leaves from twelve pecan trees throughout the 2021 and 2022 growing seasons. The fungal microbiome was curated from these leaves, using internal transcribed spacer region sequencing. Results showed that fungicides impacted the pecan leaf community in the late 2021 season, while there was no significant effect in the 2022 season. Filamentous fungi like *Sclerotiniaceae* appeared to be more affected by fungicide applications, while yeast-like fungi including *Filobasidium* sp. and *Bullera* sp. were more resilient to disturbances.

This chapter is written for the intended publication into *Phytobiomes*

Severance, B.M., Noel, Z.A., 2024. Diversity and effects of fungicides on the pecan phyllosphere microbiome. *Phytobiomes*.

Introduction

Fungicides are imperative for pathogen control but may provide deleterious effects to non-target community members. With the potential for commercial fungicides to cause non-target effects, knowledge of disturbance ecology becomes useful. Early definitions of disturbance ecology can be attributed to Bender et al. from a 1984 publication. In this manuscript, perturbations could be either 1) pulsed or a short-term sudden change in a community that recovers after, or 2) press, a continuous disturbance that causes permanent damage. In the presence of a disturbance (natural disaster, fungicide application, etc.), one of four scenarios can occur: resistance, resilience, redundancy, and regime shift (Shade, 2023). Resistance involves maintaining the structure and function of the microbial community, resilience involves structure and function that both recover, redundancy recovers function but retains an altered structure, and regime shift involves a permanently modified function. These terms echo the original definitions in 1984 but add more clarity in areas where scientists may have needed it (Glasby et al., 1996).

Previous research has studied microbiome recovery after a one-time fungicide application to corn and soybean (Noel et al. 2022). Noel noticed significant non-target effects on yeast taxa that co-occurred with potentially beneficial bacteria. While fungicides are necessary for controlling *V. effusa*, they also may alter the populations of other non-target organisms, which may change their interactions, leading to an altered community function. These altered community functions may be prone to future pathogen colonization or resilient to future disturbances. Therefore, studying microbiome alteration upon fungicidal disturbance is vital for agricultural resilience.

Corn and soybean are annual crops, and while studying disturbance against them is helpful, it leaves the door open for study on perennial crops. To date, blueberries (Lloyd et al., 2021) and

grapes (Perazzolli et al., 2014), and apples (Glenn et al., 2015) are some of the only perennial crops studied in a similar light. Like annual crop studies, Lloyd et al. concluded that fungi are significantly affected by fungicides, while bacteria are not significantly affected (2021). They also concluded that the fungicide prothioconazole may have a less deleterious effect on crop symbionts, which may be an alternative to more broad-spectrum chemicals (Lloyd et al., 2021).

Another challenge of microbiome research in the field is that many environmental factors cannot be controlled. Redford et al. (2009) explored bacterial succession on a leaf's surface throughout a growing season and determined that controlling various environmental factors across temporal space was difficult, if not impossible. Despite these challenges, the phyllosphere should be studied to determine the effects of chemical applications. Pecan offers a unique lens through which to view these issues, as it is a perennial crop that endures intense fungicide pressure each year.

Pecans (*Carya illinoinensis*) are a prized agricultural crop native to the United States, generating $399 million in 2020 (NASS). The phenolic compounds from their shells have even been shown to provide antitumor activity (Hilbig et al., 2018). However, as with most commercial crops, pecan trees are not immune to pathogens. Pecan scab is the most prevalent pecan disease, and scab infection can significantly affect yield, as it is the most devastating pecan disease in the southeastern United States (Demaree, 1924). Pecan scab is caused by a fungus called *Venturia effusa* G. Winter, previously known by the anamorphic name *Fusicladium effusum* (Winter et al., 2022).

V. effusa falls under the phylum Ascomycota, class Dothideomycetes (Winter et al. 2022). Despite over one hundred years of previous research, a sexual cycle for this species had not been described until 2019 (Charlton et al.). Current challenges in studying the epidemiology of pecan

scab are related to a limited understanding of survival structures and habitats in leaf litter and multiple morphologically similar organisms like *Mycosphaerella* (Charlton et al., 2019). Therefore, more research should be done to elucidate these topics. Because of current limitations, *V. effusa* must be controlled on pecan trees to secure a hearty crop.

Pecan scab causes disease by forming lesions that proliferate on young leaves in mid- to late-April; these lesions will move to the nuts if allowed residence into August. Fungicide applications are recommended to start and end at these times to mitigate scab presence as much as possible (UGA Extension, 2016). If not controlled, yield can be little to none, and the quality of the nuts will not be acceptable for commercial use. Susceptible cultivars require ten to twelve sprays to provide a proper yield. These factors can give sufficient scab control, but their effects on the other microbes living on leaves are unknown.

Over two years, we explored the pecan phyllosphere bacterial and fungal communities, sprayed with fungicides typically applied to pecans commercially. As previously observed, we hypothesize that fungicides, including non-pathogenic yeast species, will significantly affect the fungal community structure. We will study alpha and beta diversity and differential abundance to accomplish this goal and determine species co-occurrences using network dynamics.

Materials and Methods

Sample site and management. Leaf samples were collected from Auburn University's E.V. Smith Research Station Plant Breeding Unit (PBU) in Tallassee, Alabama (AAES, 2020). This unit contains a pecan (*Carya illinoinensis*) orchard with Desirable and Elliot cultivars on which the experiment was conducted. Fungicide applications of Phostrol®, Stratego® YLD, SUPER

TIN 4L (2021), Absolute® Maxx, Miravis® Top, and Elast (2022) were performed at recommended label rates and are described in detail in Table 1.

Fungicide applications. In 2021, the fungicide Phostrol® (Nufarm 2018) was applied to the pecan orchard at a rate of 40 fl oz acre^{-1}. Phostrol® contains the active ingredient phosphorous acid salts which targets phosphonates (FRAC, 2024). The Stratego ® YLD fungicide (Bayer CropScience 2021) contains the active ingredients trifloxystrobin and pyraclostrobin, which target complex III of fungal respiration and C14-demethylation in sterol biosynthesis, respectively. Stratego ® YLD was applied at a rate of 10 fl oz acre^{-1}. SUPER TIN 4L is a fungicide that contains the active ingredient triphenyltin hydroxide. Triphenyltin hydroxide is an inhibitor of oxidative phosphorylation and targets ATP synthase (FRAC, 2024). SUPER TIN 4L was applied to the pecan orchard at a rate of 12 fl oz acre^{-1}. In 2022, the fungicide Absolute® Maxx (Bayer CropScience, 2019) was applied to the pecan orchard at a rate of 7.67 fl oz acre^{-1}. Absolute® Maxx contains the active ingredients tebuconazole (a triazole) and trifloxystrobin (Bayer CropScience, 2019). Triazoles target C14-demethylase in sterol biosynthesis (FRAC, 2024). Trifloxystrobin is a quinone outside inhibitor in FRAC Group 11 (FRAC, 2024). Elast (Arysta LifeScience, 2017) is a fungicide that contains the active ingredient dodine, which has the proposed mode of action of cell membrane disruption (FRAC, 2024). Elast was applied to the pecan orchard at a rate of 25 fl oz acre^{-1}. In 2022, Phostrol® and SUPER TIN 4L were also applied at the same rate as the previous year. Miravis® Top (Syngenta, 2019) was also applied in 2022 at a rate of 13.6 fl oz acre^{-1}. Miravis® Top contains active ingredients pydiflumetofen—a succinate dehydrogenase inhibitor—and difenoconazole—a triazole demethylation inhibitor—, which are in FRAC groups 7 and 3, respectively (Syngenta, 2019; FRAC, 2024).

Sample collection.

In 2021, pecan leaf samples were collected at six time points, with one compound leaf being taken per treatment per time point from six replicate trees. The branches sampled throughout the experiment were marked with flagging tape to ensure the same area was sampled each time. The first sampling occurred before the first fungicide application on 28 April 2021 denoted as T1. The second sampling occurred nine days post fungicide (dpf) with an application of propiconazole and trifloxystrobin, and the third sampling occurred 16-dpf following the first application (T2 and T3). Similarly, after the second fungicide application of propiconazole and trifloxystrobin in 2021, which occurred on 14 May 2021, we sampled seven dpf, and 14-dpf (T4 and T5). Then, we sampled 21-dpf after the third fungicide spray, triphenyltin hydroxide mixed with phosphorus acid salts. In 2022, pecan leaf samples were collected at eight time points. The first sampling occurred before the first fungicide application on 15 April 2022; the second was 12-dpf, the third was 14-dpf, the fourth was 11-dpf, the fifth was six dpf, the sixth was 12-dpf, the seventh was 18-dpf, and the final sampling was 15-dpf. Leaves were sampled from a test branch that was sprayed with fungicide, and a control branch that was blocked from fungicide application using a plastic bag (Figure 1). To test the effect of the bag itself on the phyllosphere microbiome, leaves were sampled from trees not sprayed with fungicides plus or minus a bag placed over the branch were sequenced. The inclusion of the bag did not significantly affect diversity of fungi (Table 2).

Sampling, DNA extractions, library preparation, sequencing, bioinformatics, and analysis were performed with previously described methods (Longley et al., 2020; Lundberg et al., 2013; Bowsher et al., 2021). Pecan leaves were sampled by removing one compound leaf from each branch. A flamed metal hole punch, washed in 70% ethanol, and flame sterilized using a butane

torch between samples, was used to obtain one 6 mm leaf disk from a random spot on each leaflet of the compound leaf. These leaf disks were punched directly into a 2 mL microcentrifuge tube with a 4 mm sterile ball bearing containing 500µL of CSPL buffer (Omega Bio-Tek, Norcross, GA, USA). Samples were placed on ice and returned to the lab, where they were stored in a freezer at -80°C until DNA extraction could be performed. Throughout the growing season, leaves were sampled from the bottom canopy (~10 ft above ground) due to a lack of equipment to reach higher and because spray equipment may have difficulty reaching the top canopy of the tree. Plant tissues were ground up using a TissueLyser II (Qiagen Inc., Germany), and total DNA was extracted with a Mag-Bind® Plant DNA Plus kit (Omega Bio-Tek, Norcross, GA, USA). DNA extraction was also performed from tubes containing no leaf punches as a negative control and sequenced alongside other samples. A positive sequencing control was included for the fungal or prokaryote library. A 12-member synthetic mock community was used as a positive control for fungi (Palmer et al., 2018), and the Microbial Community DNA Standard was used as a positive control for prokaryotes (Zymo Research, California, USA).

Fungal and prokaryote sequencing. Amplicon library preparation for ITS and 16S community profiling. Amplicon libraries were prepared from a modified three-step PCR protocol (Tables 6, 7, and 8). The fungal library was constructed around the ITS region and was amplified using primers ITS1F and ITS4. A bacterial library was built to target the V4 region of the 16S rRNA gene using primers 515F and 806R. Amplicon libraries were purified with a SequalPrep™ Normalization Plate Kit (Thermo Fisher Scientific, USA) and then pooled and concentrated with Amicon® Ultra 0.5mL Centrifugal Filters (MilliporeSigma, Germany). The library was then purified and was size-selected plus with 0.7X AMPure XP magnetic beads (Beckman Coulter

Inc., California, USA). Amplicon libraries were run on a 1% gel to ensure the library was clean of primer dimers. Amplicon libraries were then paired-end sequenced on an Illumina MiSeq 2x300 bp V3 chemistry (Illumina, USA) and demultiplexed by SeqCenter (Pittsburg, PA). Raw fungal sequences are available in the Sequence Read Archive (SRA) under BioProject PRJNA1117508.

Bioinformatic sequence processing. Forward and reverse prokaryote reads were merged using VSEARCH 2.22.1 (Rognes, 2016). Only forward fungal ITS1 reads were used since reverse reads do not overlap. Primers were removed using Cutadapt 1.13 (Martin, 2011). Fungal reads were trimmed to remove conserved SSU and 28S regions using VSEARCH 2.22.1. Reads were then quality filtered at an expected error threshold of less than 1.0 error per read for fungi and less than 0.5 errors per read for bacteria and truncated to equal length (fungi 263 bp; prokaryote 250 bp) using VSEARCH 2.22.1. Singletons and chimeras were removed, and de novo OTU clustering was performed at 97% similarity using VSEARCH 2.22.1 and USEARCH 11.0.667 (Edgar, 2010). Prokaryote taxonomy classification of representative OTU sequences was performed against the SILVA v138.2 database. Fungal taxonomy classification of representative OTU sequences was performed against the UNITE v9.0 eukaryote database using the Naïve Bayesian Classifier (NBC) and SINTAX algorithms. The SINTAX algorithm was run to classify mock sequences (Palmer et al., 2018), and these classifications were placed in the taxonomy that the NBC algorithm provided. OTUs unidentified at the Kingdom level, nonfungal taxa, and OTUs identified as chloroplast or mitochondria in either database were removed from further analysis.

Import and preprocessing in R. Data were imported into R 4.2.2 (R Core Team), and the packages *phyloseq* 1.44.0 (McMurdie et al., 2013) and *vegan* 2.6-4 (Okansen et al. 2022) were

used for most analyses. Samples with low sequencing coverage (< 5000 reads) were removed from the analysis. Contaminant OTUs (prevalent in negative extraction controls) were removed with the R package *decontam* 1.20.0 (Davis et al., 2017). Before normalization, richness was assessed using the 'estimate_richness' function of *phyloseq*. The results of alpha diversity analyses were plotted using 'ggplot2' 3.4.2 (Wickham, 2016). Sample read counts were normalized using the cumulative sum scaling (CSS) technique within the *metagenomeSeq* R package version 1.42.0 (Paulson et al., 2023).

Statistical analysis. Alpha diversity measures of Shannon, inverse Simpson, richness, and evenness were calculated, using 'Fungicide', 'Time', and 'Cultivar' as fixed effects and analysis was separated by year. An ANOVA was then run on the measurements to test for significance. Shannon, inverse Simpson, and richness were calculated for the filtered samples using the 'estimate_richness' function of the *phyloseq* R package. Pielou's evenness was calculated by dividing the Shannon diversity by the natural log of richness. Beta diversity on Bray-Curtis distances was tested through permutational multivariate analysis of variance (PERMANOVA) with the 'adonis2' function using the R package *vegan* (Okansen et al., 2022). Differential abundance was calculated using the R package *DESeq2* 1.40.2 (Love et al., 2014) because it lowers the possibility of false discovery with appropriate p-value correction (Weiss et al., 2017). Network comparison was performed on the 80 taxa with the highest occupancy across all fungicide or control samples by using the 'filtTax' function equal to 'highestFreq' = 80 within NetCoMi 1.1.0 (Peschel, 2023) from networks initially constructed using SPRING (Yoon et al., 2019), which estimates associations between OTUs. Normalization of read counts and zero handling were performed in SPRING. Statistics for the network, such as calculating eigenvector

centrality, closeness centrality, betweenness centrality, and positive edge percentage, were calculated. Nodes were identified as hubs if eigenvector centrality values were above the 95% quantile of the distribution. Data files and scripts used for this analysis are available on GitHub (https://github.com/Beatrice-Severance/Pecan_Phyllosphere_Amplicon_Sequencing).

Results

General statistics. Once fungal reads were filtered, 1915 OTUs and 20,543,268 reads remained. The average read depth was 55,522 sequences (Figure 2). Regarding the bacterial reads, the PNA clamps used for library preparation failed to block the amplification of mitochondria and plastid DNA in 2021, and comparison of samples was not appropriate due to low sequence depth (4300 reads per sample) after filtering contaminants. Therefore, the following analysis only deals with fungi. Rarefaction curves (Figure 3) plateaued as the average read depth was reached, indicating that the fungal communities on pecan leaves were adequately sampled.

Alpha diversity. Shannon, inverse Simpson, richness, and evenness were calculated for the filtered samples using the 'estimate_richness' function of the *phyloseq* R package. ANOVA values are displayed in Table 3. ANOVA information for the 2021 Shannon index shows that time significantly altered fungal diversity ($p = 0.01286$). In 2022, the Shannon index shows that time was significant ($p < 0.001$). The interaction of fungicide and cultivar was also significant ($p = 0.03606$). Similarly, a comparison for the 2021 inverse Simpson index shows that time was significant ($p < 0.001$). Time remained a significant factor for richness in 2021 and 2022 and evenness in 2021 and 2022 ($p < 0.001$). Richness was significantly hindered in the fungicide treatment at T4 in 2021 ($p = 0.0047$). Richness measurements were plotted and are shown in Figure 4. Evenness measurements also showed significance for cultivar and the interaction of

fungicide and time, with p-values of 0.01684 and 0.03065, respectively. Evenness measurements for 2022 showed significance for the fungicide and time interaction, with a p-value of 0.04261.

Beta diversity. PERMANOVA was run to compare fungal composition (Tables 4 and 5). Since time was a significant driver of differences in fungal diversity, we ran separate comparisons for each time point. For 2021, this was run for six different time points, T1 through T6 (Table 4). For T1, fungicide had significance for beta diversity, with a p-value of 0.043. For T2, the fungicide and cultivar interaction showed significance, with a p-value of 0.007. For T4 and T5, fungicide had significance, with p-values of 0.034 and 0.012, respectively. For T6, significance was observed, with a p-value of 0.001. Principle coordinates analysis for 2021 T4-T6 is displayed in Figure 5.

For 2022, PERMANOVA was run for eight different time points, T1 through T8 (Table 5). No significance was observed for any time point except for T8, where the fungicide and cultivar interaction were significant, with a p-value of 0.023. This is in contrast to 2021, when the effect of fungicides was observed at several time points.

Differential abundance analysis. DESeq2 was used to calculate differential abundance for times four through six (T4 to T6) in 2021 since those showed a clear effect of fungicide on the composition (Figure 6). Filamentous fungi OTUs like *Sclerotiniaceae* (FOTU_70) and *Ramularia* sp. (FOTU_1 and FOTU_1792) were more abundant in the non-treated control samples, indicating that fungicide applications affected these populations in the treatment groups. Yeast OTUs *Filobasidiaceae* (FOTU_14 and FOTU_182), *Bullera alba* (FOTU_7), *Vishniacozyma heimaeyensis* (FOTU_5 and FOTU_2533), *Rhodotorula babjevae* (FOTU_41), and *Sporobolomyces* (FOTU_26) were significantly more abundant in fungicide-treated groups,

indicating that these yeasts may be naturally resilient to fungicide applications and/or take up space that is made available after fungicides hinder the growth of traditional filamentous fungi.

Network analysis. A co-occurrence network containing control and fungicide treatments over 2021 and 2022 was generated using SPRING and displayed with NetCoMi (Figure 7). Fungal OTUs represented in both treatments were displayed; if an OTU was absent in one treatment, it was not shown in the network. Statistics for the network indicated that the centrality of the networks changed due to the fungicide treatment. For example, eigenvector centrality was significant, with a p-value of 0.0056. Closeness centrality had a p-value of 0.025, and betweenness centrality had a p-value of 0.058. The positive edge percentage decreased from 98.35% in the control network to 95.72% in the fungicide network, though the difference was not significant (p-value = 0.662). Filamentous fungi typically associated as pathogens like *Sclerotinia* sp. (FOTU_70), *Ramularia* sp. (FOTU_1 and FOTU_1792), and *Fusicladium effusum* (FOTU_29), the pecan scab pathogen, were located on the periphery of both networks. FOTU_7—*Bullera alba*—was a central hub to the control and fungicide networks, indicating that the yeast may play an essential role in the phyllosphere community overall and was not significantly affected by fungicide applications. In addition, the fungicide network contains hubs (eigenvector centrality greater than 95% of the distribution) like *Vishniacozyma tephrensis* (FOTU_1816), *Cyphellophora* sp. (FOTU_142), and *Tricellula* sp. (FOTU_37), indicating that fungicide applications may destabilize phyllosphere communities and cause more subcommunities with hub taxa. In the control network, *Stagonosporosis* sp. (FOTU_122), *Tilletiopsis lilacina* (FOTU_39), and Didymellaceae (FOTU_6) were additional hubs.

Discussion

Our study aimed to understand fungicidal disturbances in a perennial crop system with high disease pressure over time. This objective was unique since recent studies have done similar things in annual crops, which receive fungicides applied directly to the foliage less frequently than the eight to ten fungicide applications annually to combat the highly destructive fungal pathogen *V. effusa.* The comparison of fungal diversity in 2021 is consistent with the hypothesis that fungicides significantly affect the microbiome since control and fungicide treatments diverged from each other over time. Additionally, phyllosphere yeasts were more abundant in fungicide-treated samples, which aligns with other studies showing that fungicides alter phyllosphere yeasts' abundance. Finally, we observed that yeasts were central to the pecan phyllosphere networks, demonstrating their potential importance to network structure. Lastly, we observed that network centrality is disturbed when fungicides are applied, indicating that fungicides disrupt the co-occurrence patterns of fungi in the phyllosphere, potentially altering community function.

Reasons to explain beta diversity differences could be seasonal variation, resistance, or resilience of microbiome members. A study attempted to determine a leaf surface's bacterial succession and stated that controlling various environmental factors across temporal space was difficult, if not impossible (Redford et al., 2009). In addition, variability between trees on a single date was more similar than a single tree over time. This study suggested that the reason was frequent disturbance events and multiple succession sequences may occur throughout a season. This seasonal variation aspect, as well as numerous fungicide disturbances, may hinder the ability to make conclusions on the effects that fungicides truly have on the community and could aid in the explanation for why beta diversity was not significant in both 2021 and 2022.

Our findings are consistent with previous research that states that phyllosphere yeasts are significantly abundant after fungicide sprays, while filamentous pathogenic fungi are lowered in these fungicide-treated groups. Our differential abundance displays phyllosphere yeast taxa Filobasidiaceae, *Bullera alba*, *Vishniacozyma heimaeyensis*, and *Rhodotorula babjevae* emerging as significantly abundant in fungicide treatments compared to controls for T4-T6 in 2021

Network analysis shows that centrality is disturbed when fungicides are applied, altering the abundance of core members and causing microbiome competition. It has been reported that high levels of disturbance can reduce cooperation (Brockhurst et al., 2010), potentially altering network centrality. A member of the Sclerotiniaceae family increased in number of associations in the fungicide network, most being positive. Fungicides could decrease the quantity of fungi on a phyllosphere leaf, Sclerotiniaceae may have the potential to co-occur with other central members of the community due to this new spatial dynamic. In addition, with *V. tephrensis* becoming a hub and *B. alba* maintaining its central role in the fungicide network, this may indicate that yeasts become more abundant after fungicide treatments and may help stabilize communities that have been disturbed.

Overall, fungicides are expected to cause a disturbance in localized microbiomes, and the phyllosphere is no exception. Fungicides affected the pecan phyllosphere differently each year; significantly in 2021 according to principal coordinate analyses, with yeast species becoming significantly more abundant under conditions, but no difference in 2022. This inconsistency could be due to seasonal variation or the fact that the specific fungicides applied were not the same each year. Despite this lack of consistent significance, network structure was shifted due to factors that should be further explored. Since yeast populations remained prevalent in fungicide-

treated communities, it is imperative that more study be put into the function of these organisms, as they may provide more information on the overall functions of phyllosphere community as well as plant health promotion in general. These results help improve understanding of a high disease pressure perennial crop system and effects that fungicide disturbances can cause.

Future research for this chapter can involve running NetCoMi on just T4-T6 in 2021, since this would likely provide significant values for hub or centrality shifts. In addition, disease severity data has been recorded but not previously used and should be incorporated for more comprehensive analysis. Finally, bacterial data can be incorporated to study indirect effects of fungicides on the pecan phyllosphere microbiome but requires re-sequencing in 2021 due to previous complications. Overall, these data can provide the extra context that would make the chapter more complete.

Table 1. Fungicide applications with respective dates of applications and sampling.

Year	Spray number	Date applied	Date sampled	DPF	Product	Rate per hectare (mL/ha)	Active Ingredient
2021	-	-	28-Apr-2021--T1	0-dpf	-	-	-
2021	1	28-Apr-2021	07-May-2021--T2	9-dpf	Stratego	700.53	propioconazole + trifloxystrobin
2021	1	28-Apr-2021	14-May-2021--T3	16-dpf	Stratego	700.53	propioconazole + trifloxystrobin
2021	2	14-May-2021	21-May-2021--T4	7-dpf	Stratego	700.53	propioconazole + trifloxystrobin
2021	2	14-May-2021	04-Jun-2021--T5	14-dpf	Stratego	700.53	propioconazole + trifloxystrobin
2021	3	04-Jun-2021	25-Jun-2021--T6	21-dpf	Phostrol/Supertin 4L	2802.13/840.64	phosphorous acid salts + triphenyltin hydroxide
2022	-	-	15-Apr-2022--T1	0-dpf	-	-	-
2022	1	15-Apr-2022	27-Apr-2022--T2	12-dpf	Phostrol	2802.13	phosphorous acid salts
2022	2	29-Apr-2022	13-May-2022--T3	14-dpf	Phostrol	2802.13	phosphorous acid salts
2022	3	16-May-2022	27-May-2022--T4	11-dpf	Absolute Maxx	537.31	tebuconazole + trifloxystrobin
2022	4	27-May-2022	02-Jun-2022--T5	6-dpf	Supertin 4L/Elast	840.64/1751.33	triphenyltin hydroxide + dodine
2022	4	27-May-2022	09-Jun-2022--T6	12-dpf	Supertin 4L/Elast	840.64/1751.34	triphenyltin hydroxide + dodine
2022	5	12-Jun-2022	30-Jun-2022--T7	18-dpf	Miravis Top	952.72	adepidyn + difenoconazole
2022	6	30-Jun-2022	15-Jul-2022--T8	15-dpf	Supertin 4L/Elast	840.64/1751.34	triphenyltin hydroxide + dodine

In 2021, surfactants of Scanner and Top Surf were applied at 0.25%. Chelated zinc was added at 1qt/acre. The insecticide Advise 2FL was applied at a rate of 448.34mL/ha. In 2022, the surfactants Humispread and Preference were applied at the recommended rate of 1120.85mL/ha each. Amazing Zinc was used as a fertilizer, at a rate of 1120.85mL/ha. The insecticides Advise 4 and Advise 2FL were applied both at a rate of 224.17mL/ha, and the insecticides Intrepid Edge and Closer were applied at 448.34mL/ha and 192.65mL/ha, respectively.

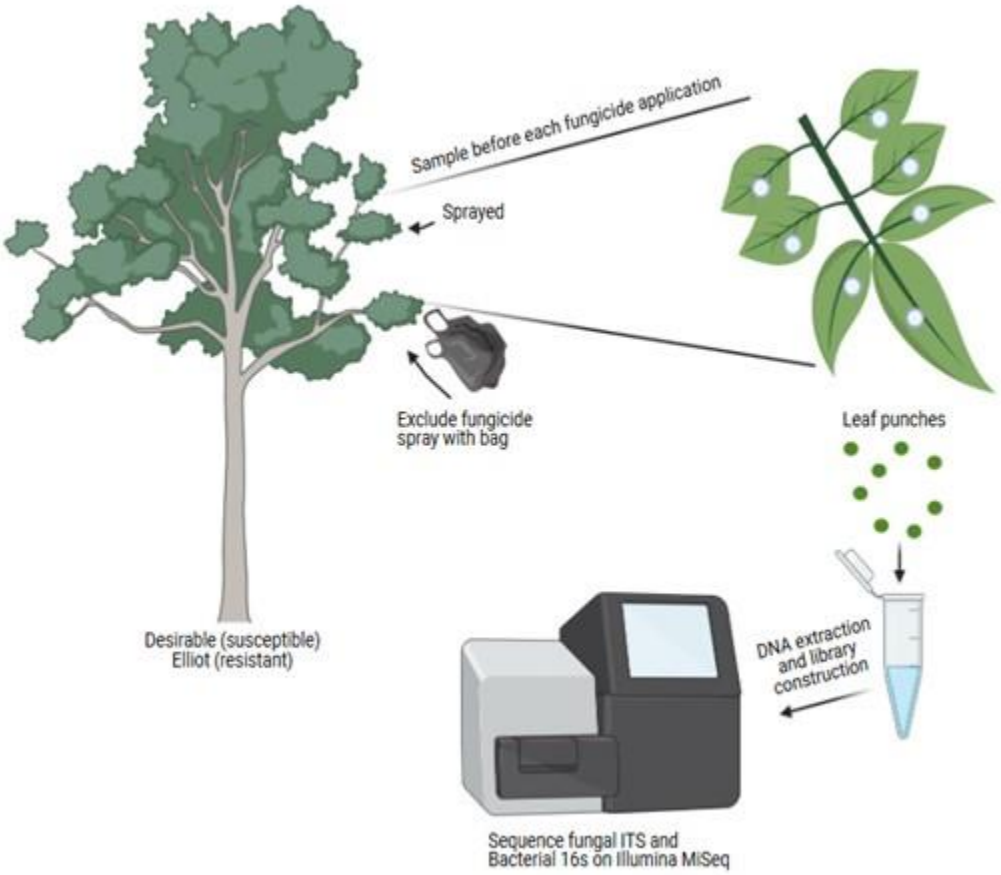

Figure 1. Pecan orchard sampling methods. At each time point, compound leaves were taken from a fungicide-treated branch and an unsprayed control branch (bagged before application and removed after), and a sterilized hole punch took leaf disks from each leaflet before placing them in a 2mL microcentrifuge tube with DNA extraction buffer. DNA extraction was performed, and ITS and 16S were sequenced on an Illumina MiSeq.

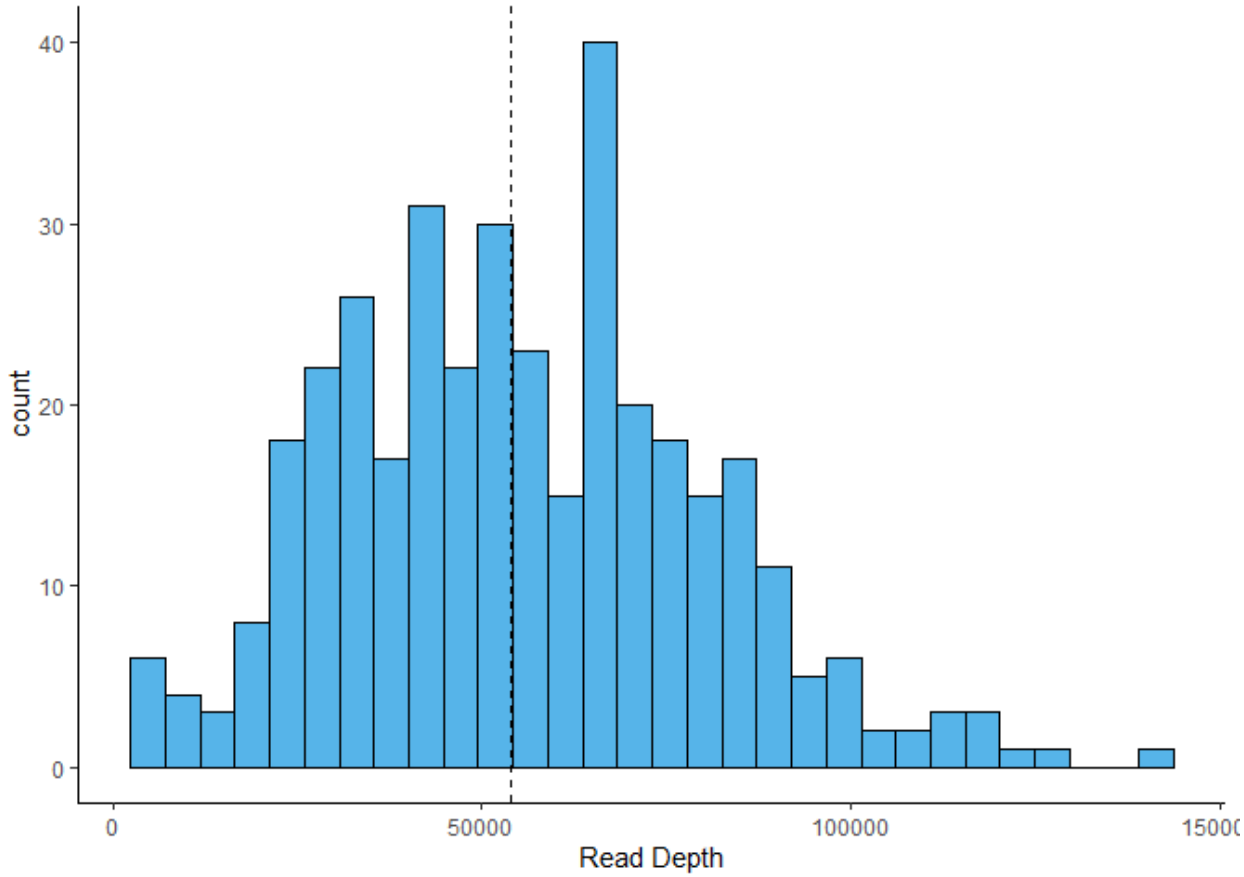

Figure 2. Read depth for fungal sequences obtained in 2021 and 2022. Sequences were filtered by removing negative controls, subsetting samples to Kingdom Fungi, and removing samples with less than 5000 reads before being displayed. The dotted line represents the median sequence read depth of just over 50,000 reads per sample.

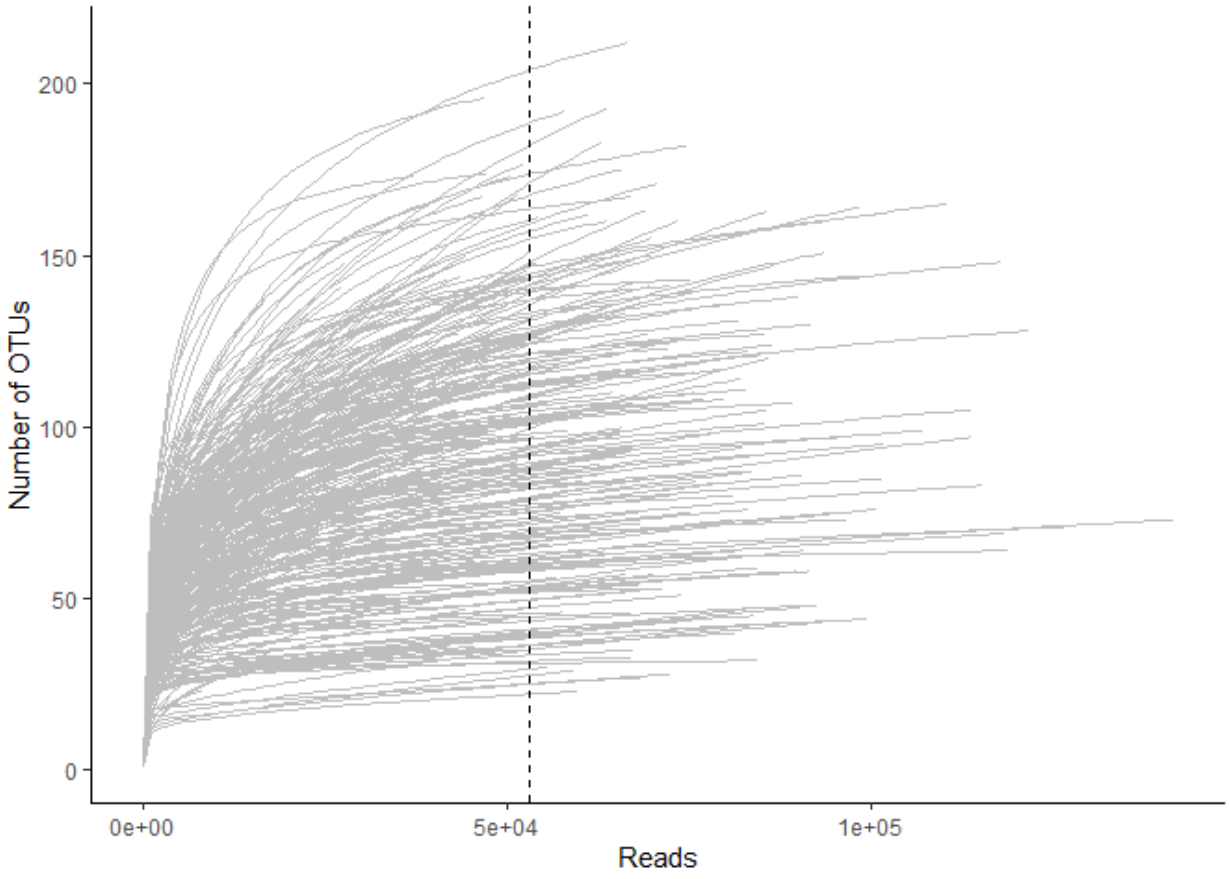

Figure 3. Rarefaction curves for filtered leaf samples. The dotted line represents the median read depth.

Table 2. ANOVA tables to show that bagging had no confounding effect on pecan orchard sampling. The bagging effect was traced through the first three fungicide applications of 2021 and 'DateSampled' was the only significant effect, which was expected.

Factor	Degrees Freedom	Sum of Squares	R^2	Pseudo-F	P
Bagged	1	0.083	0.019	0.872	0.493
DateSampled	2	1.111	0.257	5.857	0.001
Bagged x DateSampled	2	0.281	0.065	1.479	0.130
Residual	30	2.846	0.659	-	-
Total	35	4.320	1	-	-

Table 3. ANOVA tables for alpha diversity measurements.

Year	Response	Factor	Degrees Freedom	Sum of Squares	R^2	Pseudo-F	P
2021	Shannon	Fungicide	1	0.024	0.024	0.493	0.484
		Time	5	0.734	0.147	3.041	0.013
		Cultivar	1	0.043	0.043	0.895	0.346
		Fungicide x Time	5	0.221	0.044	0.917	0.473
		Fungicide x Cultivar	1	0.010	0.010	0.200	0.656
		Time x Cultivar	5	0.212	0.042	0.877	0.499
		Fungicide x Time x Cultivar	5	0.249	0.050	1.032	0.402
		Residuals	117	5.650	0.048	-	-
2022	Shannon	Fungicide	1	0.025	0.025	0.260	0.611
		Time	7	10.367	1.481	15.700	< 0.001
		Cultivar	1	0.002	0.002	0.018	0.894
		Fungicide x Time	7	1.190	0.170	1.801	0.090
		Fungicide x Cultivar	1	0.422	0.422	4.469	0.036
		Time x Cultivar	7	0.315	0.0450	0.477	0.851
		Fungicide x Time x Cultivar	7	0.728	0.104	1.102	0.364
		Residuals	161	15.189	0.094	-	-
2021	Inverse Simpson	Fungicide	1	8.311	8.311	3.559	0.062
		Time	5	55.267	11.054	4.733	< 0.001
		Cultivar	1	2.228	2.228	0.954	0.331
		Fungicide x Time	5	8.968	1.794	0.768	0.575
		Fungicide x Cultivar	1	1.618	1.618	0.693	0.407
		Time x Cultivar	5	19.644	3.929	1.682	0.144
		Fungicide x Time x Cultivar	5	17.646	3.529	1.511	0.192
		Residuals	117	273.219	2.335	-	-
2022	Inverse Simpson	Fungicide	1	0.001	0.001	0.001	0.976
		Time	7	105.491	15.070	12.345	< 0.001
		Cultivar	1	0.111	0.1106	0.091	0.764
		Fungicide x Time	7	9.921	1.417	1.161	0.328
		Fungicide x Cultivar	1	2.954	2.954	2.420	0.122
		Time x Cultivar	7	6.169	0.881	0.722	0.654
		Fungicide x Time x Cultivar	7	8.065	1.152	0.944	0.475
		Residuals	161	196.543	1.221	-	-
2021	Richness	Fungicide	1	519.000	519.400	1.074	0.302
		Time	5	118439	23687.80	48.993	< 0.001
		Cultivar	1	1107	1107.3	2.290	0.133
		Fungicide x Time	5	5312	1062.5	2.198	0.059
		Fungicide x Cultivar	1	1074	1073.7	2.221	0.139

		Time x Cultivar	5	2095	418.900	0.867	0.506
		Fungicide x Time x Cultivar	5	1963	392.6	0.812	0.543
		Residuals	117	56569	483.5	-	-
2022	Richness	Fungicide	1	2130	2130.4	2.294	0.132
		Time	7	79645	11377.8	12.251	< 0.001
		Cultivar	1	3112	3111.9	3.351	0.069
		Fungicide x Time	7	4429	632.7	0.681	0.688
		Fungicide x Cultivar	1	433	433.5	0.467	0.495
		Time x Cultivar	7	2717	388.1	0.418	0.890
		Fungicide x Time x Cultivar	7	703	100.4	0.108	0.998
		Residuals	161	149524	928.7	-	-
2021	Evenness	Fungicide	1	0.007	0.007	2.861	0.093
		Time	5	0.110	0.022	9.260	< 0.001
		Cultivar	1	0.014	0.014	5.881	0.017
		Fungicide x Time	5	0.030	0.006	2.564	0.031
		Fungicide x Cultivar	1	0.000	0.000	0.204	0.653
		Time x Cultivar	5	0.019	0.004	1.640	0.155
		Fungicide x Time x Cultivar	5	0.013	0.003	1.108	0.360
		Residuals	117	0.277	0.002	-	-
2022	Evenness	Fungicide	1	0.000	0.000	0.119	0.731
		Time	7	0.611	0.087	21.047	< 0.001
		Cultivar	1	0.008	0.008	1.949	0.165
		Fungicide x Time	7	0.034	0.005	1.169	0.323
		Fungicide x Cultivar	1	0.017	0.017	4.177	0.042
		Time x Cultivar	7	0.017	0.002	0.582	0.770
		Fungicide x Time x Cultivar	7	0.027	0.004	0.930	0.485
		Residuals	161	0.667	0.004	-	-

Table 4. PERMANOVA values for each time point in beta diversity analysis in 2021.

Year	Time	Factor	Degrees Freedom	Sum of Squares	R^2	Pseudo-F	P
2021	T1	Fungicide	1	0.257	0.084	2.073	0.043
		Cultivar	1	0.156	0.051	1.261	0.235
		Fungicide x Cultivar	1	0.151	0.050	1.217	0.278
		Residual	20	2.479	0.815	-	-
		Total	23	3.043	1	-	-
2021	T2	Fungicide	1	0.205	0.049	1.279	0.249
		Cultivar	1	0.089	0.021	0.557	0.687
		Fungicide x Cultivar	1	0.712	0.169	4.440	0.007
		Residual	20	3.207	0.761	-	-
		Total	23	4.214	1	-	-
2021	T3	Fungicide	1	0.070	0.062	1.477	0.165
		Cultivar	1	0.083	0.073	1.757	0.115
		Fungicide x Cultivar	1	0.035	0.031	0.749	0.609
		Residual	20	0.944	0.834	-	-
		Total	23	1.132	1	-	-
2021	T4	Fungicide	1	0.226	0.106	2.428	0.034
		Cultivar	1	0.073	0.034	0.783	0.544
		Fungicide x Cultivar	1	0.154	0.072	1.656	0.139
		Residual	18	1.675	0.787	-	-
		Total	21	2.128	1	-	-
2021	T5	Fungicide	1	0.190	0.122	2.968	0.012
		Cultivar	1	0.137	0.088	2.151	0.068
		Fungicide x Cultivar	1	0.017	0.011	0.269	0.969
		Residual	19	1.213	0.779	-	-
		Total	22	1.557	1	-	-
2021	T6	Fungicide	1	0.198	0.176	4.641	0.001
		Cultivar	1	0.059	0.052	1.373	0.205
		Fungicide x Cultivar	1	0.013	0.012	0.312	0.963
		Residual	20	0.853	0.760	-	-
		Total	23	1.123	1	-	-

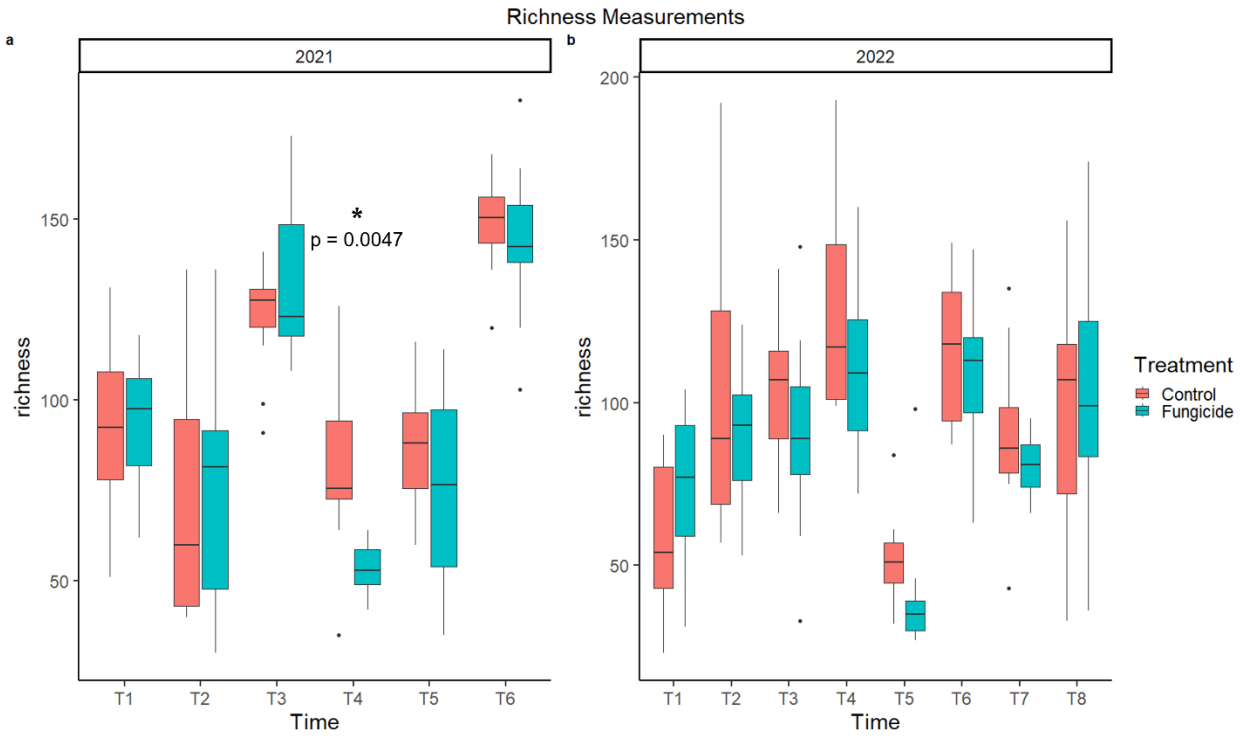

Figure 4. Fungal richness measurements for 2021 and 2022. A linear model was run with Fungicide, Time, and Cultivar as fixed effects. A post-hoc test was conducted for T4 in 2021 to determine the significant p-value of 0.0047. Treatments are in red (control) and blue (fungicide).

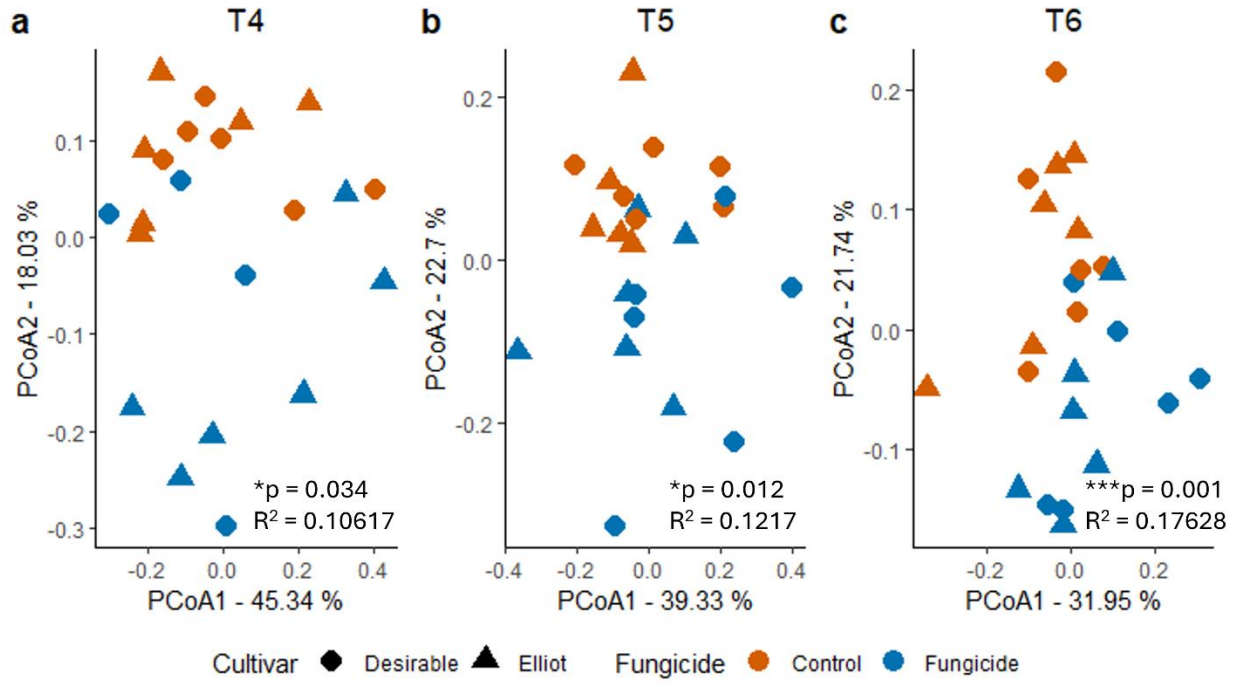

Figure 5. Principle coordinates ordinations on Bray-Curtis distances for times four through six (T4 through T6) sampled in 2021. Orange points indicate control treatments, while blue points indicate fungicide treatments. Triangles represent the Elliot cultivar, and circles represent the Desirable cultivar. Significance increases over time, indicating that the communities diverge from each other in the presence or absence of fungicides.

Table 5. PERMANOVA values for each time point in beta diversity analysis in 2022.

Year	Time	Factor	Degrees Freedom	Sum of Squares	R^2	Pseudo-F	P
2022	T1	Fungicide	1	0.176	0.056	0.974	0.406
		Cultivar	1	0.129	0.041	0.715	0.709
		Fungicide x Cultivar	1	0.147	0.047	0.817	0.591
		Residual	15	2.706	0.857	-	-
		Total	18	3.158	1	-	-
2022	T2	Fungicide	1	0.009	0.012	0.259	0.882
		Cultivar	1	0.048	0.06431	1.415	0.240
		Fungicide x Cultivar	1	0.011	0.01506	0.331	0.846
		Residual	20	0.672	0.90885	-	-
		Total	23	0.740	1	-	-
2022	T3	Fungicide	1	0.064	0.048	1.085	0.341
		Cultivar	1	0.055	0.041	0.931	0.417
		Fungicide x Cultivar	1	0.037	0.028	0.625	0.670
		Residual	20	1.175	0.883	-	-
		Total	23	1.330	1	-	-
2022	T4	Fungicide	1	0.024	0.038	0.775	0.530
		Cultivar	1	0.024	0.039	0.799	0.507
		Fungicide x Cultivar	1	0.031	0.049	1.017	0.365
		Residual	18	0.551	0.874	-	-
		Total	21	0.631	1	-	-
2022	T5	Fungicide	1	0.207	0.078	1.760	0.167
		Cultivar	1	0.252	0.096	2.143	0.107
		Fungicide x Cultivar	1	0.297	0.113	2.525	0.052
		Residual	16	1.880	0.713	-	-
		Total	19	2.635	1	-	-
2022	T6	Fungicide	1	0.075	0.043	0.951	0.395
		Cultivar	1	0.185	0.108	2.361	0.072
		Fungicide x Cultivar	1	0.044	0.025	0.556	0.699
		Residual	18	1.413	0.823	-	-
		Total	21	1.716	1	-	-

2022	T7	Fungicide	1	0.104	0.080	1.688	0.135
		Cultivar	1	0.116	0.089	1.878	0.117
		Fungicide x Cultivar	1	0.094	0.072	1.519	0.171
		Residual	16	0.988	0.759	-	-
		Total	19	1.302	1	-	-
2022	T8	Fungicide	1	0.129	0.029	1.290	0.237
		Cultivar	1	0.200	0.044	1.991	0.115
		Fungicide x Cultivar	1	0.378	0.084	3.764	0.023
		Residual	38	3.811	0.844	-	-
		Total	41	4.518	1	-	-

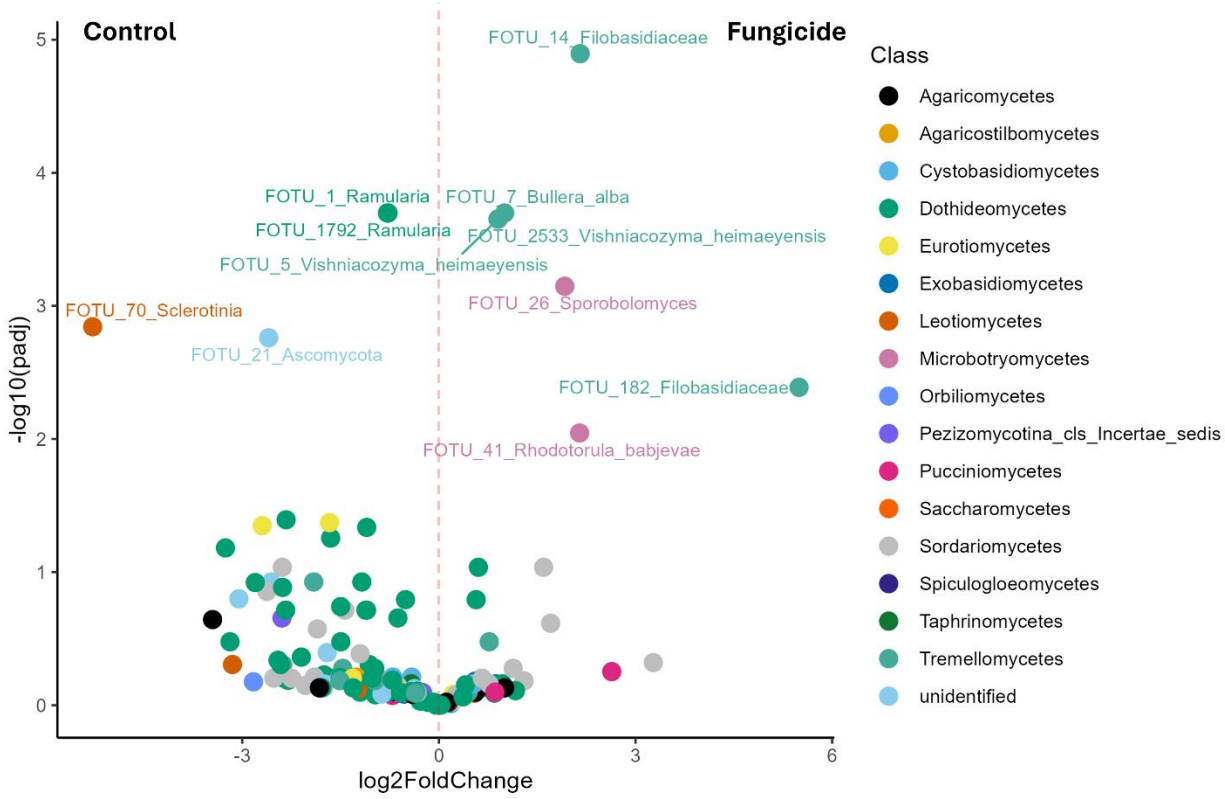

Figure 6. Differentially abundant fungal OTUs for 2021 data times 4 through 6 (T4 to T6). Fungal OTUs that were significantly more abundant in fungicide-treated samples are labeled on the right side of the graph, and fungal OTUs that were significantly more abundant in control-treated samples (no fungicides) are labeled on the left of the graph, separated by the dotted red line. Points are colored according to the fungal Class. Differentially abundant OTUs were determined in DeSeq2 ($\alpha = 0.01$). Differentially abundant taxa in the fungicide treatment include

yeast taxa, while differentially abundant taxa in the control treatment include three filamentous fungi and one unidentified Ascomycota taxa.

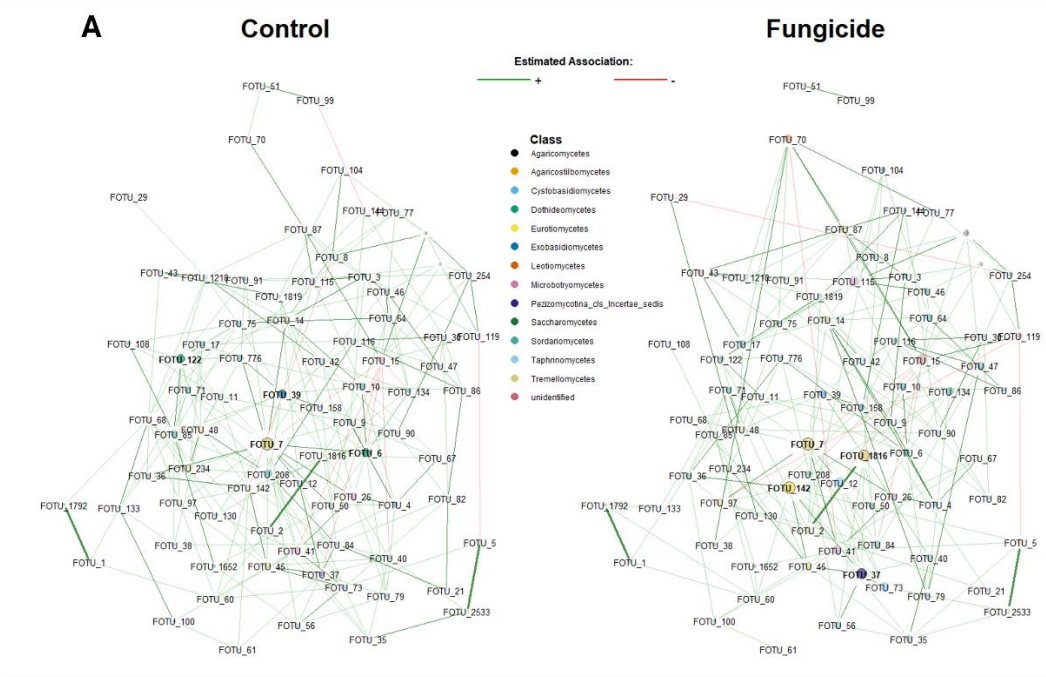

B **FOTU Identification**

FOTU	ID	Class
7	*Bullera alba*	Tremellomycetes
39	*Tilletiopsis lilacina*	Exobasidiomycetes
37	*Tricellula* sp.	Pezizomycotina cls Incertae sedis
122	*Stagonosporosis* sp.	Dothideomycetes
6	Didymellaceae	Dothideomycetes
70	*Sclerotinia* sp.	Leotiomycetes
142	*Cyphellophora* sp.	Eurotiomycetes
1816	*Vishniacozyma tephrensis*	Tremellomycetes
41	*Rhodotorula babjevae*	Microbotryomycetes
1	*Ramularia* sp.	Dothideomycetes
1792	*Ramularia* sp.	Dothideomycetes
15	unidentified fungi	unknown
29	*Fusicladium effusum*	Dothideomycetes
254	Gnomoniaceae	Sordariomycetes
14	Filobasidiaceae	Tremellomycetes

Figure 7. (A) A co-occurrence network displaying differences in connections between control and fungicide treatments over 2021 and 2022. Points are labeled with corresponding OTU and are colored according to class. Green lines indicate a positive association, while red lines indicate a negative association. (B) Notable OTUs are highlighted to give more information on taxa central to the network and/or visibly differed in the number of connections. The networks were generated using SPRING. The networks contained fungal OTUs displaying the top 80 taxa with the highest occupancy. The networks were visualized and compared using NetCoMi.

Table 6. Three step amplicon library preparation reagents and PCR master mixes. Table is adapted from Noel et al., 2022.

Plant Associated Prokaryotes		Fungi	
Reagent	**Volume per reaction (uL)**	**Reagent**	**Volume per reaction (uL)**
Step 1		**Step 1**	
2X Dream Taq Green PCR Master Mix (Thermo Fisher, USA)	6.25	2X Dream Taq Green PCR Master Mix (Thermo Fisher, USA)	6.25
10uM 515F Primer (IDT, USA)	0.375	10uM ITS 1F Primer (IDT, USA)	0.375
10uM 806R Primer (IDT, USA)	0.375	10uM ITS 4 Primer (IDT, USA)	0.375
Bovine Serum Albumin (BSA, 3%)	1	Bovine Serum Albumin (BSA, 3%)	1
50uM Mitochondrial PNA clamp 1:50 dilution (PNA Bio, USA)	0.18	H2O	3
50uM Plastid PNA clamp 1:50 dilution (PNA Bio, USA)	0.18	Extracted DNA	1
GC Enhancer (Thermo Fisher, USA)	0.64		
Extracted DNA	3		
Step 2		**Step 2**	
2X Dream Taq Green PCR Master Mix (Thermo Fisher, USA)	6.25	2X Dream Taq Green PCR Master Mix (Thermo Fisher, USA)	6
10uM 515F Primer Frameshift (IDT, USA)	0.375	10uM ITS 1F Primer Frameshift (IDT, USA)	0.3
10uM 806R Primer Frameshift (IDT, USA)	0.375	10uM ITS 4 Primer Frameshift (IDT, USA)	0.3
Bovine Serum Albumin (BSA, 3%)	0.64	Bovine Serum Albumin (BSA, 3%)	3
H2O	0.36	H2O	0.4
GC Enhancer (Thermo Fisher, USA)	2	Step 1 Product	2
Step 1 Product	2		
Step 3		**Step 3**	
2X Dream Taq Green PCR Master Mix (Thermo Fisher, USA)	8	2X Dream Taq Green PCR Master Mix (Thermo Fisher, USA)	8
Barcode Forward Primer	0.5	Barcode Forward Primer	0.5
Bovine Serum Albumin (BSA, 3%)	1	Unique 10 Nucleotide Barcode	1
GC Enhancer (Thermo Fisher, USA)	0.5	H2O	1.5
Unique 10 Nucleotide Barcode	1	Step 2 Product	4
Step 2 Product	4		

Table 7. Cycling conditions for PCR in library preparation for prokaryotes and fungi. Table is adapted from Noel et al., 2022.

Prokaryote								
Step 1			Step 2			Step 3		
Time	Temperature (°C)	Cycles	Time	Temperature (°C)	Cycles	Time	Temperature (°C)	Cycles
3:00	94		5:00	95		5:00	95	
0:15	94	25X	0:30	95	5X	0:30	95	5X
0:10	75		0:15	75		0:35	63	
0:30	50		0:30	50		0:55	72	
0:45	68		0:50	72		7:00	72	
10:00	72		7:00	72		Infinite	10	
Infinite	10		Infinite	10				

Fungi								
Step 1			Step 2			Step 3		
Time	Temperature (°C)	Cycles	Time	Temperature (°C)	Cycles	Time	Temperature (°C)	Cycles
5:00	95		5:00	95		5:00	95	
0:30	95	20X	0:30	95	8X	0:30	95	8X
0:30	50		0:35	50		0:35	50	
1:00	72		1:05	72		1:10	72	
7:00	72		7:00	72		7:00	72	
Infinite	10		Infinite	10		Infinite	10	

Table 8. Primers used for amplicon library preparation. [a]Frameshift primers are used in PCR reactions at an equal molar ratio of forward and reverse primers. Table is adapted from Noel et al., 2022.

	Prokaryote Primer Sequences		Fungal Primer Sequences	
Step 1	Sequence	Primer name	Sequence	Primer name
	GTGCCAGCMGCCGCGGTAA	515F	CTTGGTCATTTAGAGGAAGTAA	ITS 1F
	GGACTACHVGGGTWTCTAAT	806R	AGCCTCCGCTTATTGATATGCTTAART	ITS 4
		Frameshifts (combination of 6)		Frameshifts (combination of 6)
Step 2[a]				
	NNNNNNNN GA		NNNNNNNN TT	
	GTGCCAGCMGCCGCGGTAA	515F F1	CTTGGTCATTTAGAGGAAGTAA	ITS 1F F1
	NNNNTNNNN GA		NNNNTNNNN TT	
	GTGCCAGCMGCCGCGGTAA	515F F2	CTTGGTCATTTAGAGGAAGTAA	ITS 1F F2
	NNNNCTNNNN GA		NNNNCTNNNN TT	
	GTGCCAGCMGCCGCGGTAA	515F F3	CTTGGTCATTTAGAGGAAGTAA	ITS 1F F3
	NNNNACTNNNN GA		NNNNACTNNNN TT	
	GTGCCAGCMGCCGCGGTAA	515F F4	CTTGGTCATTTAGAGGAAGTAA	ITS 1F F4
	NNNNGACTNNNN GA		NNNNGACTNNNN TT	
	GTGCCAGCMGCCGCGGTAA	515F F5	CTTGGTCATTTAGAGGAAGTAA	ITS 1F F5
	NNNNTGACTNNNN GA		NNNNTGACTNNNN TT	
	GTGCCAGCMGCCGCGGTAA	515F F6	CTTGGTCATTTAGAGGAAGTAA	ITS 1F F6
	NNNNN AC		NNNNN AG	
	GGACTACHVGGGTWTCTAAT	806R F1	AGCCTCCGCTTATTGATATGCTTAART	ITS4 F1
	NNTNNN AC		NNTNNN AG	
	GGACTACHVGGGTWTCTAAT	806R F2	AGCCTCCGCTTATTGATATGCTTAART	IT4 F2
	NNCTNNN AC		NNCTNNN AG	
	GGACTACHVGGGTWTCTAAT	806R F3	AGCCTCCGCTTATTGATATGCTTAART	ITS4 F3
	NNACTNNN AC		NNACTNNN AG	
	GGACTACHVGGGTWTCTAAT	806R F4	AGCCTCCGCTTATTGATATGCTTAART	ITS4 F4
	NNGACTNNN AC		NNGACTNNN AG	
	GGACTACHVGGGTWTCTAAT	806R F5	AGCCTCCGCTTATTGATATGCTTAART	ITS4 F5

	NNTGACTNNN AC GGACTACHVGGGTWTCTAAT	806R F6	NNTGACTNNN AG AGCCTCCGCTTATTGATATGCTTAART	ITS4 F6
Step 3				
	AATGATACGGCGACCACCGAGATCT ACACGCCTCCCTCGCGCCATCAGAGA TGTG	PCR F	AATGATACGGCGACCACCGAGATCTACA CGCCTCCCTCGCGCCATCAGAGATGTG	PCR F
	Other oligos			
	GGCAAGTGTTCTTCGGA	"mPNA" Mitochondrial Blocker		
	GGCTCAACCCTGGACAG	"pPNA" Plastid Blocker		

3. CHAPTER THREE

Fungal interactions, metabolism, and phylogenomic placement of a novel phyllosphere yeast

Abstract

Phyllosphere yeasts have repeatedly been described as highly abundant species on various plant surfaces, but little has been done to study these organisms more thoroughly. Sampled from a magnolia leaf in Auburn, Alabama, isolate EMM_F3 is a novel Dothideomycete yeast that changes color from cream to dark brown or black. After sequencing, this yeast only matches 80.7% to any known relatives. We studied this yeast through various methods, involving interactions against representative fungi, elucidating metabolic properties, and placing the yeast taxonomically. A genome of EMM_F3 was sequenced, assembled, and annotated. Our fungal interactions show potential inhibition of species like *Fusarium graminearum*, involving color change on either end. Findings show that EMM_F3 is placed in the Dothideales clade, with *Delphinella strobiligena* being a sister taxon.

This chapter is written for the intended publication into *Microbiology Spectrum*

Introduction

The phyllosphere is the aerial or above-ground plant parts, including leaves, stems, flowers, and fruits (Lindow & Brandl, 2003; Knief et al., 2010). The phyllosphere encompasses almost double the amount of surface area as the total land surface area (Vorholt, 2012), indicative of massive amounts of space for various microorganisms to colonize. Despite this large space, the organisms that colonize these habitats have been historically understudied (Vorholt, 2012).

Various yeast species are common phyllosphere inhabitants. Phyllosphere yeasts have often been described as abundant globally but have yet to be described in extensive detail (Lindow & Brandl, 2003). Yeasts are the most abundant epiphytic fungal group in the phyllosphere (Inacio et al., 2002). Filamentous fungi can exist as epiphytes, but they are often dormant until finding a way to colonize endophytically (Andrews & Harris, 2000; de Jager et al., 2001). Yeast exists in several fungal phyla, but the ones in the phyllosphere primarily belong to the Basidiomycetes, including members of Microbotryomycetes and Tremellomycetes (Andrews, 1992). Ascomycete yeasts, on the other hand, are also in or on plant leaves. Specifically, certain members of this phylum like the Dothideomycete class, have much to provide to the phyllosphere environment.

The Dothideomycete class is the largest class of ascomycete fungi, encompassing 23 orders, 110 families (Wijayawardene et al., 2017), and over 19,000 species (Schoch et al., 2009). Several clades in this class also display polyphyletic genera (Wijayawardene et al., 2017), so independent evolution can occur. The class also shows extreme biodiversity, including pathogens like *Venturia effusa*—pecan scab—and *Cochliobolus heterostrophus*—southern corn leaf blight, as well as non-pathogens like endophytes, epiphytes, mycoparasites, extremophiles, lichenized

fungi and mycorrhizal fungi (Haridas et al., 2020). Despite these vastly different lifestyles, many taxa are still unclassified (Luxking & Hawksworth, 2018), perhaps even into the thousands.

While the Dothideomycete clade includes many filamentous fungi, yeasts are also present. A well-studied Dothideomycete yeast is *Aureobasidium pullulans*. This yeast is a genus characterized by melanization increasing with age, turning yellow/pink to dark brown/dark black. It can be found worldwide in various climates ranging from glaciers to desert rock (Gostincar et al., 2014). It contains the unique metabolite pullulan, known for its adhesive ability, oxygen-impermeable films, and biodegradability (Gostincar et al., 2014). These traits make the species a target for biocontrol application. Gray mold on grapes caused by *Botrytis* spp. was shown to be controlled to a significant degree when treated with *Aureobasidium pullulans* (Parafati et al., 2015), making it an ideal biocontrol for post-harvest fruit protection. Similarly, Zhang et al. (2012) observed *A. pullulans* inhibition of *Botrytis* spp. and *Monilinia laxa* (a stone fruit pathogen). In addition, commercial biocontrol products containing *A. pullulans* already exist, like Boni-Protect® and Blossom-Protect® (Weiss et al., 2006; Kunz, 2004). The Blossom-Protect® product controls fire blight caused by *Erwinia amylovora* by inducing host defenses via activation of PR gene expression (Zeng et al., 2023). The stark phenotypic change, metabolite production, and pathogen suppression all encourage the exploration of phylogenetically related yeast for similar properties.

Since *A. pullulans* is a known biocontrol yeast species, there is much potential for other yeasts to provide similar benefits. There is a current need for novel antifungal compounds in both agriculture and medicine, and the potential of yeasts to contain these compounds is promising. Yeasts may currently be underrepresented due to bias in hosts that are sampled. *Magnolia grandiflora* exists as an ornamental plant but contains much taxonomic novelty in yeast

(Wanasinghe, 2020). The first record of the yeast genus *Miera* was first isolated from Magnolia leaves in Louisiana (Rush & Aimes et al., 2013). Due to these promising aspects, the continued study of yeasts isolated from previously understudied hosts may be beneficial.

We aimed to determine whether various phyllosphere yeasts have the potential to alter the growth of fungi from three fungal phyla and one oomycete *in vitro*, indicating potential broad antifungal activity. Fifteen yeast isolates from a culture collection of 103 cultures isolated from *Magnolia grandiflora* and five isolated from *Carya illinoiensis* (Table 9) were tested against fungal isolates representing three different fungal phyla and one oomycete lineage. From these co-culture experiments, one interaction between the undescribed Dothidiomycete yeast isolate EMM_F3 and *Fusarium graminearum* PH-1 was particularly striking due to the repeated presence of a zone of inhibition and pigment changes in *F. graminearum*. Our objectives are to present the results of these initial co-culture experiments, compare the genome of EMM_F3 to other Dothideomycete genomes, and present changes in the metabolome with and without competition from *Fusarium graminearum* PH-1.

Importance

Phyllosphere yeasts exist globally, yet there is much to learn about their function on a leaf surface. Our research investigated a novel phyllosphere yeast isolated from *Magnolia grandiflora* to highlight specific functions related to fungi-fungi interactions (phenotype change and metabolome composition) and place the isolate to describe its taxonomic placement. We tested several yeast isolates against fungi representing three fungal phyla and one oomycete. Through co-culture assays *in vitro*, we discovered that EMM_F3 induces a phenotypic change in *Fusarium graminearum* PH-1—lack of red pigmentation and significantly reduced mycelial

growth. We identified metabolites undecane and nonadecane using mass spectrometry from these interactions. We also produced a draft genome of EMM_F3 and compared it to other Dothidiomycete fungi. From its genome, we could confidently place the isolate in the Dothideales clade, with the closest relative being the wheat pathogen *Delphinella strobiligena* and sharing common ancestry with *Aureobasidium pullulans*. This study helps provide a starting point for exploring environmental yeast species and a background for research on EMM_F3.

Results

EMM_F3 shows the strongest inhibitory effect against competing fungi. Primary interaction experiments on agar medium of the 20 yeasts against four three mycelial fungi and one oomycete showed that EMM_F3, EMM_F8, and EMM_F89 were the strongest inhibitors (Figure 8). They consistently had inhibition scores ranging from 2 to 4, with average ratings being 2.3335, 2.833, and 3, respectively, when interacting with *Fusarium graminearum* PH-1. This indicates that EMM_F3 and EMM_F8 both consistently produced noticeable zones of inhibition.
However, of all fungi tested, EMM_F3 was intriguing because it was the most inhibitory and more novel taxonomically than other fungi according to ITS sequencing. In particular, the interaction was *Fusarium graminearum* PH-1, which gave the most apparent inhibition zones. Therefore, we quantified the inhibition in a tissue culture plate with an insert in each well where metabolites could be exchanged through a porous membrane (0.4 μm) but kept the two fungi from physically interacting. Upon weighing the fresh weight of *F. graminearum* PH-1 in this co-culture experiment, we found that *F. graminearum* PH-1 had significantly lower mycelial growth by weight when grown wells containing EMM_F3 (t-test; $P = 0.016$). Additionally, when

growing alone, a bright red pigment was produced in *F. graminearum* compared to when grown with EMM_F3. These results are displayed in Figure 10.

EMM_F3 was grown on a solid agar medium in a bisected plate with competitor PH-1 on the other side of the partition to explore the possibility of volatile compounds in the inhibition observed. This experiment was run in triplicate, with results shown in Figure 9. PH-1 growth did not appear inhibited by EMM_F3 volatiles, as the size was not visibly different from the control. However, a statistical comparison of colony size could not be completed because there was only one control plate. Collectively, these co-culture experiments support the hypothesis that EMM_F3 was producing a secreted metabolite capable of inhibiting fungal growth *in vitro*, especially towards *F. graminearum* PH-1.

Mass Spectrometry reveals unique metabolites with antimicrobial properties. We performed untargeted gas chromatography with mass spectroscopy (GC/MS) of EMM_F3 interacting with *F. graminearum* PH-1 and compared it to EMM_F3 or *F. graminearum* PH-1 growing alone. We used three extraction methods (Acid FAMES, Base FAMES, and Acetylation). Raw data from the Auburn University Mass Spectrometry Center identified 299 metabolites. We determined that several metabolites were unique to EMM_F3 or the interaction, indicating that it was only produced in the presence of EMM_F3. Metabolites that were identified unique to EMM_F3 were Met78 (tridecane), Met212 (nonadecane), and Met215 (nonadecane). Metabolites identified only in the presence of EMM_F3 but remained of unknown identity were Met35, Met37, Met247, and Met97 (Figure 11).

Comparative Genomics. EMM_F3 raw genome had 2,858,439,152 base pairs (bp) sequenced with a Q > 30 (92.14%). The final assembly was 24,166,584 bp long and contained 123 contigs greater than or equal to 500 bp. The N50 was 334,563 and GC content was 54.39%. 7730 proteins were predicted from the genome. 1282 complete BUSCOs (97.7%) were matched when choosing Dikarya as the comparison. When choosing Dothideomycetes for a deeper comparison, 3581 complete BUSCOs (94.6%) were matched. AntiSMASH detected 22 regions coding for biosynthetic gene clusters, with seven matching a similar known cluster: clavaric acid, an antitumor terpene matching 100%; scytalone, a melanin biosynthesis T1PKS that matched 40%; ankaflavin, a T1PKS that matches 12%; metachelin, an NRPS siderophore that matched 37%; choline, a cell signaling NRPS-like cluster that matched 100%, putisolvin, an antiadhesive RiPP-like cluster that matched 25%; and APE Vf, an arylpolyene antioxidant that matched 10%. These AntiSMASH results are listed in Table 10. Dothideomycete genomes were taken from JGI and compared to EMM_F3 (Table 11). Transcription factors (TFs) predicted from these genomes are listed in Figure 12. EMM_F3 did not contain the largest count in any TF category but did contain more helix-loop-helix DNA-binding domains (14) than most, third only to *C. minteri* (20) and *F. fulva* (15). Zinc knuckle motifs (11) were also high in EMM_F3, second only to *A. pullulans*, *F. fulva*, and *P. eumusae* (12). In contrast, EMM_F3 contained fewer Fungal-specific TF domains (59) than other species, outranking only *D. strobiligena* (54) and *A. pullulans* (52). Clusters of Orthologous Genes (COGs) are displayed in Figure 13. EMM_F3 contained fewer COGs in Carbohydrate transport and metabolism (419) compared to D. strobiligena (456) and A. pullulans (624). Similarly, secondary metabolites biosynthesis, transport and catabolism counts (338) are low in EMM_F3 compared to *D. strobiligena* (376) and *A. pullulans* (396). Finally, EMM_F3

had 484 counts for posttranslational modification, protein turnover, and chaperones, which is low compared to neighbors (*D. strobiligena*: 512; *A. pullulans*: 531).

Finally, the maximum likelihood tree was generated using protein sequences based on 500 single-copy orthologous genes among the Dothideomycete genomes selected (Figure 14). EMM_F3 fell within a clade containing other melanized yeast-like taxa *Delphinella strobiligena* and *Aureobasidium pullulans*, demonstrating a morphologically consistent clade. It was sister to *D. strobilignea* despite having 85% similarity when running the genome through BLAST. The outgroups *Colletotrichum sublineola* and *Pyricularia oryzae* were taken from the Sordariomycetes class and were the most basal members of the tree. Topology was similar to what was previously reported by Haridas (2020), with six monophyletic groups representing six orders of Dothideomycetes. Bootstrap values were all 100 and were based on 100 iterations.

Discussion

Phyllosphere yeasts are found worldwide, but their roles on leaf surfaces are poorly understood. We tested multiple yeast isolates against fungi from three different fungal phyla and an oomycete. Then we narrowed our focus on a new Dothidiomycete phyllosphere dimorphic fungus isolated from *Magnolia grandiflora* to uncover its specific functions, especially in fungi-fungi interactions (changes in phenotype and metabolome composition), and to determine its taxonomic classification. Evidence suggested that EMM_F3 repeatedly inhibited the mycelial growth of *Fusarium graminearum* PH-1 through secreted metabolites, not volatiles. We putatively identified tridecane and nonadecane using mass spectrometry from these interactions. We also sequenced the draft genome of EMM_F3 and compared it to other Dothidiomycete fungi. This analysis placed EMM_F3 within the Dothideales clade, closely related to the wheat

pathogen *Delphinella strobiligena* and sharing a common ancestry with *Aureobasidium pullulans* with a history of biocontrol properties. This study serves as a foundation for further research on environmental yeast species and provides a background for future studies on EMM_F3.

Fungi compete for space via various methods (Sridhar, 2019). Contact-independent methods involve volatile or diffusible compounds that inhibit the growth of competitors without needing to interact with the competitor directly. Contact-dependent methods involve physical interaction between the fungus and its competitor, involving growth in the shared space and occupying it before the competitor can establish itself. Parasitic interactions can also occur, where the fungi will replace the competitor's mycelium after making contact (Rodriguez et al., 2009). Initially, contact-dependent forms of competition were analyzed in the fungi-fungi interactions experiment. Yeasts were able to inhibit fungi, with a highlight on *Fusarium graminearum* PH-1, as PH-1 changed color from cream to a red pigment. This red pigment is likely aurofusarin/rubrafusarin (AUR), a mycotoxin known to affect egg quality in chickens (Dvorska et al. 2001; Medentsev et al. 1993), but it also possesses some antimicrobial activity (Sondergaard et al. 2016). In culture, aurofusarin has been negatively correlated with vegetative growth. When production of aurofusarin is removed due to a knockout in regulatory transcription factor GIP2, mycelia grow faster. In contrast, when GIP2 is overexpressed, aurofusarin is overproduced and mycelial growth is slower than the wild type (Kim et al., 2006). Aurofusarin production is reported in the original fungi-fungi interactions, indicating that contact-dependent methods induce the production of this metabolite. However, in the cell-insert plate experiments, the production of this pigment is no longer present when interacting with yeast EMM_F3. This could be due to specific metabolites that EMM_F3 produces to inhibit the growth of PH-1 and delay the onset of secondary metabolite aurofusarin production. However, if lack of the

aurofusarin output causes increased mycelium growth, then the PH-1 in the cell-insert experiment should show a larger wet weight. Because PH-1 produces AUR and can undergo uneven growth on the PDA media type, the cause of inhibition in PH-1 for the initial fungi-fungi interactions may be difficult due to the inconsistency of these factors.

Tridecane and nonadecane were the metabolites identified in EMM_F3 by GC-MS. Tridecane is an alkane found naturally in the southern green shield bug (Todd, 1989) and stink bugs (Krall et al., 1999) for the purpose of defense mechanisms. It is not known whether tridecane and nonadecane produced by EMM_F3 are meant to serve similar purposes, but these functions are worth noting and can be further explored through targeted GC-MS if desired. While not known, the nonadecane produced by EMM_F3 may be a derivative of nonadecanoic acid, a known fungal metabolite that is an intermediate in the breakdown of n-icosane which has been shown to inhibit cancer growth (PubChem). The ability of EMM_F3 to produce this molecule could again be confirmed through targeted GC-MS and could potentially have broad-reaching uses in the medical field if this metabolite can be produced in high amounts by the isolate.

Confirming the placement of EMM_F3 into the Dothideomycetes is important because it classifies one of the thousands of previously undiscovered/unclassified fungi by providing a metabolomic profile and comparative genomics analysis. From our analysis, EMM_F3 could potentially be a novel pine pathogen since it matches closely to *Delphinella strobiligena*. However, this does not necessarily indicate pathogenic nature, as even *D. strobiligena* is not always predicted to be a pathogen but rather was predicted as a saprobe by Haridas in a machine learning program used to identify lifestyles of Dothideomycetes (2020). In addition, a BLAST search of EMM_F3's genome against *D. strobiligena* only provided an 85.11% similarity match,

indicating that the two species are still vastly different from one another. This could mean that EMM_F3 is part of a new family, though more research would need to be done to confirm this conclusion. Nevertheless, EMM_F3 encompasses novelty even after a broad comparative genomics placement into the Dothideomycetes class. It is also worth noting that EMM_F3 was placed closely to *A. pullulans*, a yeast that contains relatives that are extremophiles, saprobes, and pathogens alike in addition to being included in known biocontrol products. Thus, EMM_F3 may be of interest for further study, and this research encourages future discovery in the field.

Future research for this chapter can involve expanding the number of Dothideales genomes for comparison since that was where EMM_F3 was placed. This can include multiple isolates and species of *Aureobasidium pullulans* in addition to other notable species in the clade. Finally, data surrounding CAZymes exists and can be incorporated in order to further support the COGs data that has been previously interpreted. Overall, these data can help the chapter feel more complete.

Materials and Methods

Mycelial fungi and yeast isolates. We used twenty environmental yeast initially isolated from the leaves of *Magnolia grandiflora* and *Carya illinoinensis* in Alabama. *Magnolia grandiflora* was chosen for its associated fungal richness and diversity associated with leaves (Wanasinghe et al., 2020). Yeast from two phyla, six subphyla, and six classes were tested against three fungi from three different phyla and one oomycete to determine if any yeast could inhibit other fungi from divergent ancestry. *Globisporangium irregulare*, isolate OEO_O28 (Oomycetes), *Rhizoctonia solani*, isolate R-12 (Basidiomycota), *Fusarium graminearum*, isolate PH-1

(Ascomycota), and *Mortierella elongata*, isolate NVP5 (Mucoromycota). The yeast isolates chosen and their taxonomic classification are listed in Table 9.

Co-culture experiments. The 20 yeast isolates and competing mycelial fungi were stored at -80ºC in 25-50% glycerol and initially grown on potato dextrose agar (1X PDA; 24 g Difco™ potato dextrose broth, 17g agar) for 72 hours. Then, a single yeast colony was placed into twenty test tubes containing 5 mL potato dextrose broth with 1 g yeast extract powder (PDB+; 24 g Difco™ potato dextrose broth, 1 g yeast extract powder, MP Biomedicals, Ohio, USA). PDB+ media was inoculated alone in a test tube as a control. Tubes were placed on a New Brunswick Excella E24 shaking incubator (Eppendorf, Germany) at 250 rpm for 72 hr at 28°C. Plugs of competing mycelial fungi were placed on 1X PDA while fungi plates were incubated at the same temperature. After 72 hr, EMM_F3 and PH-1 were plated: a 10 µL aliquot of yeast was plated on one side of the bisected plate and spread with a loop, and a 5 mm plug of PH-1 was plated on the other side (Figure 8). After inoculation, three replicate 100 mm petri dishes for each interaction were all placed in a 28°C incubator in a random pattern, and data was recorded at 72 hr post-inoculation.

Observations of interactions were recorded on a 1-5 scale, adapted from Gdanetz & Trail (2017). The scale was as follows: 1) ZOI with pigment produced in mycelial fungus, 2) ZOI with no pigment produced in mycelial fungus, 2) No ZOI; deadlock between two competitors, 3) mycelial fungus grew over of yeast, 4) yeast grew over the mycelial fungus. The experiment was completed twice. Based on this initial co-culturing experiment, one yeast (EMM_F3) was repeatedly more inhibitory than others across different fungal lineages. It was likely taxonomically novel since its ITS sequence only shared 87.9% similarity to other known fungi.

To further quantify the inhibitory phenotype observed, we quantified the difference in fungal biomass with the coculture in broth separated by a permeable membrane. This experiment focused on EMM_F3 interaction with *F. graminearum* PH-1, because it displayed the most apparent inhibition when grown on agar in the presence of the competing yeast. Both fungi were grown as previously described. *F. graminearum* was grown on 1/2X PDA for 72 hours, and EMM_F3 was grown in 5 mL potato dextrose broth (PDB) for 72 hours. Then a 0.5 mm plug from PH-1 was inoculated at the top and 10 µL of EMM_F3 at the bottom of six well tissue Costar® culture plates with 24 mm diameter inserts with a 0.4 µm pore size (Corning Incorporated, ME, USA). These inserts bisect the wells and allow chemical exchange in the broth medium while restricting the two fungi from physically interacting. One milliliter of 1X PDB was added to triplicate wells for each treatment. One well containing only EMM_F3, PH-1, or PDB was used as a control. The tissue culture plates were placed on a titer plate shaker (Lab-Line Instruments, India) at speed four and incubated at room temperature for five days with ambient light. After incubation, the plug and attached mycelium of *F. graminearum* PH-1 was placed in a 1.5 mL microcentrifuge tube, blotted dry on a towel, and a wet weight was taken. The weight of the mycelium was compared to mycelial growth without EMM_F3 in a two-sample t-test.

Bisected Plate Experiment. The co-culture experiment revealed that EMM_F3 could inhibit the mycelial growth of fungi from different phylogenetic backgrounds. Therefore, EMM_F3 was tested on a bipartite plate to determine the contribution of volatiles in the interaction. EMM_F3 and competing mycelial fungi were grown on PDA, and the bisected plate also consisted of this medium. Then, the yeast was grown on one side of the partition, and one of four fungi (OEO-

O28, PH_1, R_12, NVP5) was grown on the other so they could only interact through volatile compounds. Petri dishes were incubated at 26ºC for three days. After incubation, images of each Petri dish were taken, and the colony area with and without EMM_F3 was estimated by tracing the colony size with ImageJ.

GC-MS Preparation. To explore the yeast metabolites when interacting with *F. graminearum*, we performed gas chromatography-mass spectroscopy (GC/MS) of the wells in the cell-insert plate described previously. The cell inserts would allow chemical exchange and secreted metabolites through the 0.4 μm filter but restrict the physical interaction of the two organisms, eliminating the possibility of contact-dependent inhibition mechanisms. Metabolites from the broth in the top well (where *F. graminearum* PH-1 was growing) were prepped by passing the 1 mL through a 0.2 μm filter. After the PDB was filtered, the cell insert membrane was removed, and 750 μL of broth from the bottom of the plate (where the yeast was growing) was added to a 1.5 mL microcentrifuge tube. The tube was centrifuged at 4000 rcf for 30 minutes, and the supernatant was added to a new 1.5 mL microcentrifuge tube, leaving the pellet undisturbed. Two wells of each interaction and one well for each fungus growing alone were sampled after five days of incubation at room temperature (28 ºC) on a microplate shaker set to setting 4.

Derivation of Secondary Metabolites. The 500 μL samples were then extracted using the FAMEs Synthesis protocol (Ichihara and Fukubayashi, 2010) to extract long-chain fatty acids. FAMEs synthesis was also done under pH of 10 rather than 3 to extract basic compounds. In addition, acetylation was also performed to derive some highly hydroxylated compounds, such as sugars (Baker et al., 1994). For this reaction, acetic anhydride (24X the weight of the sample) was

added to each sample. Samples were vortexed and incubated at room temperature (26℃) for 15 minutes. Finally, 30 µL of an internal yeast standard (TruQuant Yeast Extract, IROA Technologies, Michigan) was added to each sample to characterize common metabolites, following the manufacturers' workflow (IROA Technologies, Michigan).

GC-MS Sample Processing. The samples were submitted as a 1:1 mixture of hexane and chloroform to the Auburn University Mass Spectrometry Center and stored at -80°C. An Agilent 8890 GC and 5977 MS with an Agilent HP-5MS UI column (20 m, 0.18 mm ID, 0.18 µm df) was used to analyze the samples. The temperature of the injection port was 280, and 1 µL of the sample was injected in splitless mode with a septum purge of 20 mL/min at 1.5 min. The flow was constant at 1.4 ml/min with hydrogen gas pressure at 1.4 psi. The GC oven temperature was programmed with an initial temperature of 35 °C for 4 min, ramped to 320 °C at 12 °C/min, and held for 3 min, thus requiring a total run time of 30.5 min. The MS transfer line was set at 310°C. The MS source was set to 230°C, and the EI was set to 70 eV emission with a scan range of 43 to 500 mz. The raw data was created using Agilent Enhanced ChemStation software and analyzed with MSDial (Tsugawa et al., 2015) using the Kovats RI library for the identification of metabolites (https://systemsomicslab.github.io/compms/msdial/main.html#MSP).

GC-MS Data Analysis. The peak areas for the blank samples were averaged and then subtracted from every sample. Then, internal standard-only samples were averaged and then subtracted from every sample. The remaining data was input into RStudio 4.2.2 (R Core Team) for analysis. The R packages *phyloseq* 1.44.0 (McMurdie et al., 2013) and *vegan* 2.6-4 (Okansen et al., 2022) were used to process combined metadata files with the ability to subset extracted metabolites to

focus on metabolites unique to EMM_F3. Metabolites that were unique to EMM_F3 were plotted using 'ggplot2' 3.4.2 (Wickham, 2016), separated by extraction type.

Comparative Genomics. In addition to the competition experiments, a draft genome of EMM_F3 was generated and compared to other Dothidiomycete fungi. Total genomic DNA was extracted via cetrltrimethylammonium bromide extraction. Sample libraries were prepared using the Illumina DNA Prep kit and IDT 10bp UDI indices, and sequenced on an Illumina NovaSeq 6000, producing 2x151bp reads. Demultiplexing, quality control and adapter trimming was performed with bcl-convert (v4.0.3). Illumina NovaSeq 6000 (Illumina, USA). The raw forward and reverse sequences are available on the Sequence Read Archive (SRA) under BioProject PRJNA1117874. BBDuk (https://jgi.doe.gov/data-and-tools/software-tools/bbtools/bb-tools-user-guide/bbduk-guide/) was used to remove adapters from raw reads, trim reads and check for the removal of PhiX. After this, FastQC version 0.10.1 (https://www.bioinformatics.babraham.ac.uk/projects/fastqc/) was used to assess read quality. The assembly was performed using SPAdes version 3.15.5 (Bankevich et al., 2012) and decontaminated using FCS-GX version 0.5.0 (Astashyn et al., 2024). Once the assembly was complete and decontaminated, QUAST version 5.2.0 (Gurevich et al., 2013) assessed assembly statistics. BUSCO version 5.4.3 (Manni et al., 2021) determined genome assembly and annotation completeness. AntiSMASH fungal version 7.0 (Blin et al., 2023) was utilized to determine potential biosynthetic gene clusters.

EMM_F3 was preliminarily classified as a member of the class Dothideomycete based on a comparison of the ITS sequences. Thus, 22 repeat-masked genome assemblies were downloaded, taken from the Dothideomycete clade in the Mycocosm (Grigoriev et al., 2014)

section of the Joint Genome Institute website (JGI, California, USA). These genomes were selected to cover a broad range of families within the class, ideally capturing the many functions it can offer (saprobes, extremophiles, and pathogens; Table 10). Two genomes from the Sordariomycetes class (*Pyricularia oryzae* 70-13 and *Colletotrichum sublineola* TX430BB) were used as outgroups. All genomes were used in gene prediction using a program called funannotate version 1.8.13 (https://github.com/nextgenusfs/funannotate). Before gene prediction, the program was used to clean, sort, and repeat mask genome assembly for EMM_F3. The 'clean' function uses minimap2 (Li, 2018) to look for duplicated contigs and remove them. The 'sort' function renames output files according to NCBI submission rules. The 'mask' function calls tantan (Frith, 2011) and repeat masks the genome to aid prediction. The 'predict' function trains *ab-initio* gene predictors Augustus and GeneMark, and then runs Evidence Modeler to generate consensus gene models. After genes were predicted, programs InterProScan5 version 5.66 (Jones et al., 2014) and EggNOG-Mapper version 2.1.7 (Cantalapiedra et al., 2021) were used to provide functional analysis of protein sequences and annotate orthologs on novel sequences, respectively. Next, functional annotation was performed on all genomes using the 'annotate' function of funannotate. The 'annotate' function takes InterProScan5 and EggNOG-Mapper output, and the 'predict' function output to annotate genomes. Finally, comparative genomics was performed on the output of the 'annotate' function with the 'compare' function of funannotate, which used IQ-TREE (Minh et al., 2020) to provide a maximum likelihood tree based on 500 single-copy orthologous genes. Bootstrap values are based on 100 iterations. The maximum likelihood tree was edited using iTOL v6 (Letunic & Bork, 2024). The pipeline for read processing, assembly, and annotation is located on https://github.com/Beatrice-Severance/Genome_Assembly.

Table 9. Classification of yeast cultures isolated from *Magnolia grandiflora* and *Carya illinoinensis* based on internal transcribed spacer region (ITS) sequencing. Yeast cultures were identified using GenBank.

		GenBank classification			
Isolate Code	Host	Taxonomic affiliation	Accession Number	Percent Identity	Query Coverage
EMM_F1	*Magnolia grandiflora*	Fellomyces penicillatus CBS 5492	KY103409.1	100	99
EMM_F3	*Magnolia grandiflora*	Dothidea eucalypti CBS 143417	NR_156390.1	87.9	98
EMM_F5	*Magnolia grandiflora*	Sakaguchia melibiophila JCM 8162	NR_174883.1	81.6	100
EMM_F8	*Magnolia grandiflora*	Cystobasidium raffinophilum CBS 15509	NR_174780.1	98.6	100
EMM_F9	*Magnolia grandiflora*	Dioszegia catarinonii CBS 10051	NR_155061.1	99	98.3
EMM_F12	*Magnolia grandiflora*	Meira nashicola CBS 117161	NR_119391.1	96.8	97
EMM_F16	*Magnolia grandiflora*	Debaryomyces fabryi strain CBS 789	MK394103.1	99.6	100
EMM_F22	*Magnolia grandiflora*	Filobasidium mali CBS 15651	MK050347.1	96.3	99
EMM_F25	*Magnolia grandiflora*	Vishniacozyma pseudopenaeus CBS 15472	MK050333.1	100	99.3
EMM_F42	*Magnolia grandiflora*	Hannaella pagnoccae CBS 11142	NR_155180.1	99.5	100
EMM_F43	*Magnolia grandiflora*	Symmetrospora coprosmae CBS 7899	NR_073317.1	99.6	100
EMM_F46	*Magnolia grandiflora*	Bulleromyces albus CBS 500	KY101811.1	100	100
EMM_F49	*Magnolia grandiflora*	Sporobolomyces koalae CBS 10914	KY105518.1	100	100

EMM_F58	*Magnolia grandiflora*	Derxomyces nakasei CBS 9746	KY103331.1	97.2	100
EMM_F60	*Magnolia grandiflora*	Symmetrospora proteacearum BRIP 45084	NR_174932.1	100	97
EMM_F65	*Carya illinoinensis*	Sporobolomyces shibatanus CBS 16043	CBS 16043_ex97286_ITS	100	100
EMM_F70	*Carya illinoinensis*	Erythrobasidium hasegawianum CBS 8253	AF444522	96.36	100
EMM_F74	*Carya illinoinensis*	Vishniyacozyma carnescens CBS 10755	KY105815	100	100
EMM_F79	*Carya illinoinensis*	Bullera alba CBS 500	KY101811	100	100
EMM_F89	*Carya illinoinensis*	Cryptococcus magnus UOA/HCPF 12688B	UOA/HCPF 12688B_ITS	100	100

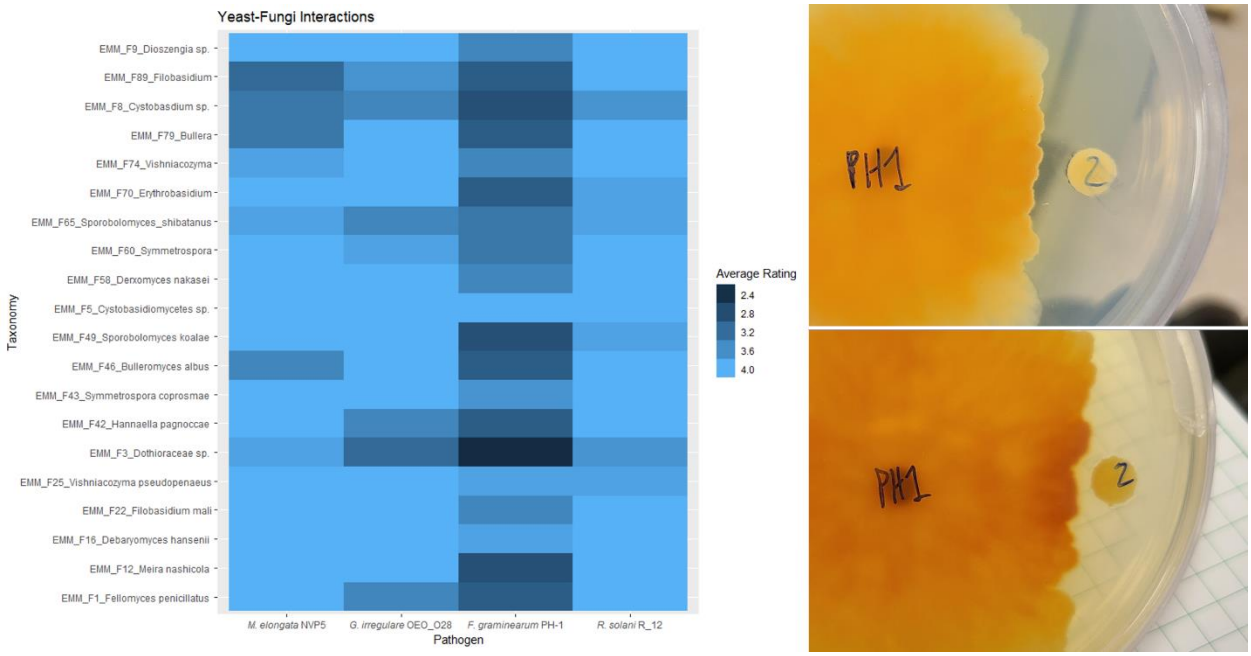

Figure 8. Heat map representing results of yeast-fungi interactions. Ratings were on a 1-5 scale, with conditions as follows: 1-Zone of inhibition (ZOI) with pigment; 2-ZOI with no pigment; 3-No ZOI (mycelium deadlock); 4-Fungi grow over top of yeast; 5-Yeast grow over fungi. The rating scale is adapted from Gdanetz & Trail (2017). Darker colors indicate a greater effect by yeast. *Fusarium graminearum* isolate PH-1 showed more phenotypic change overall compared to other fungi tested, with examples of 2 ratings to the right of the heat map.

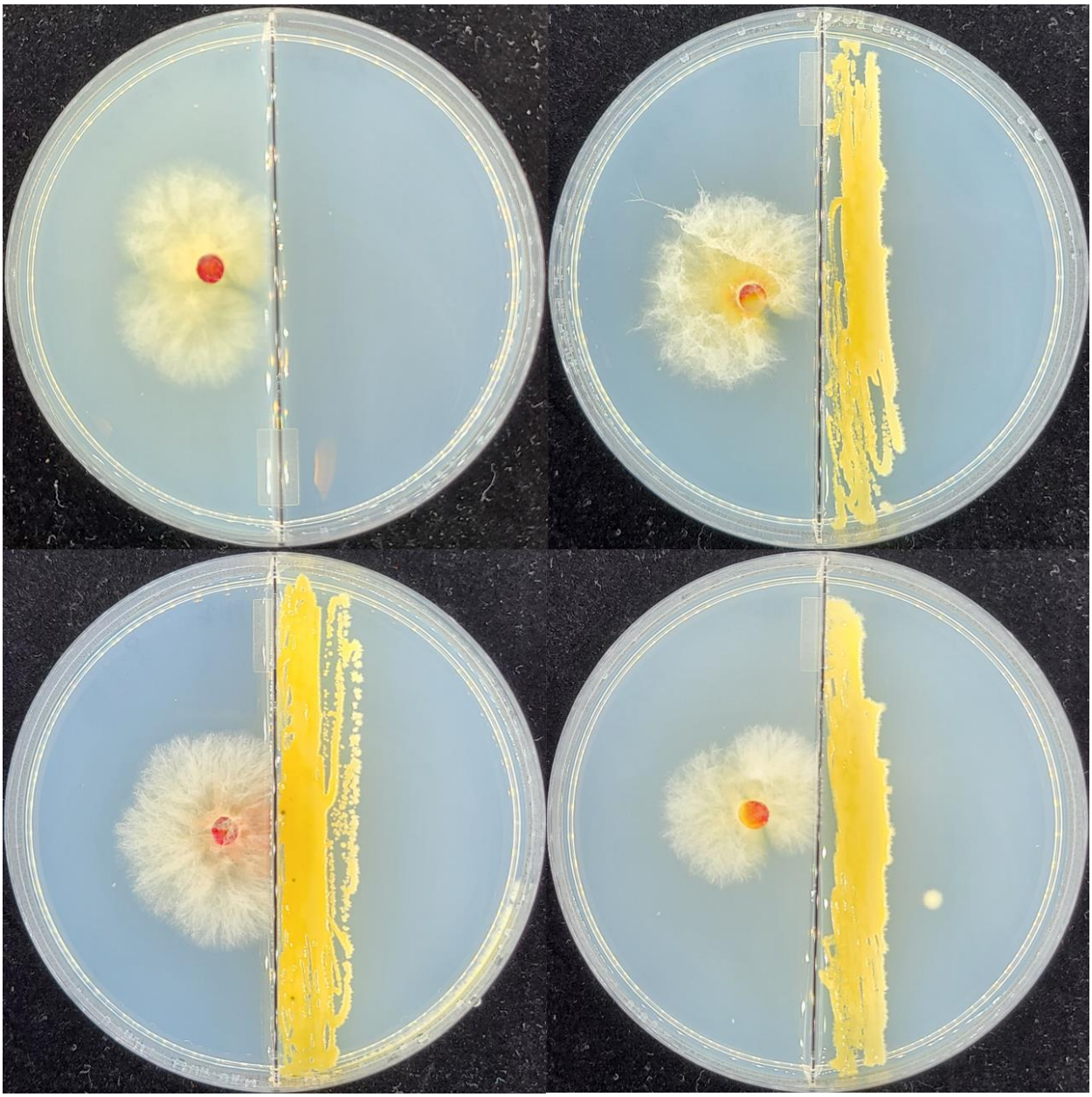

Figure 9. EMM_F3 interacting with *Fusarium graminearum* PH-1 on a bisected plate to check for volatiles. PH-1 is alone in the top left, and three replicates of PH-1 and EMM_F3 are displayed in the top right, bottom left, and bottom right. EMM_F3 was loop-inoculated on the right of each plate near the division, in order to provide an opportunity to release volatiles that may inhibit PH-1 growth on the left. PH-1 colony with and without EMM_F3 was estimated by tracing the colony size with ImageJ. EMM_F3 did not have an inhibitory effect on the fungi, as all fungi grow to the plate division without a reduction in mycelial growth.

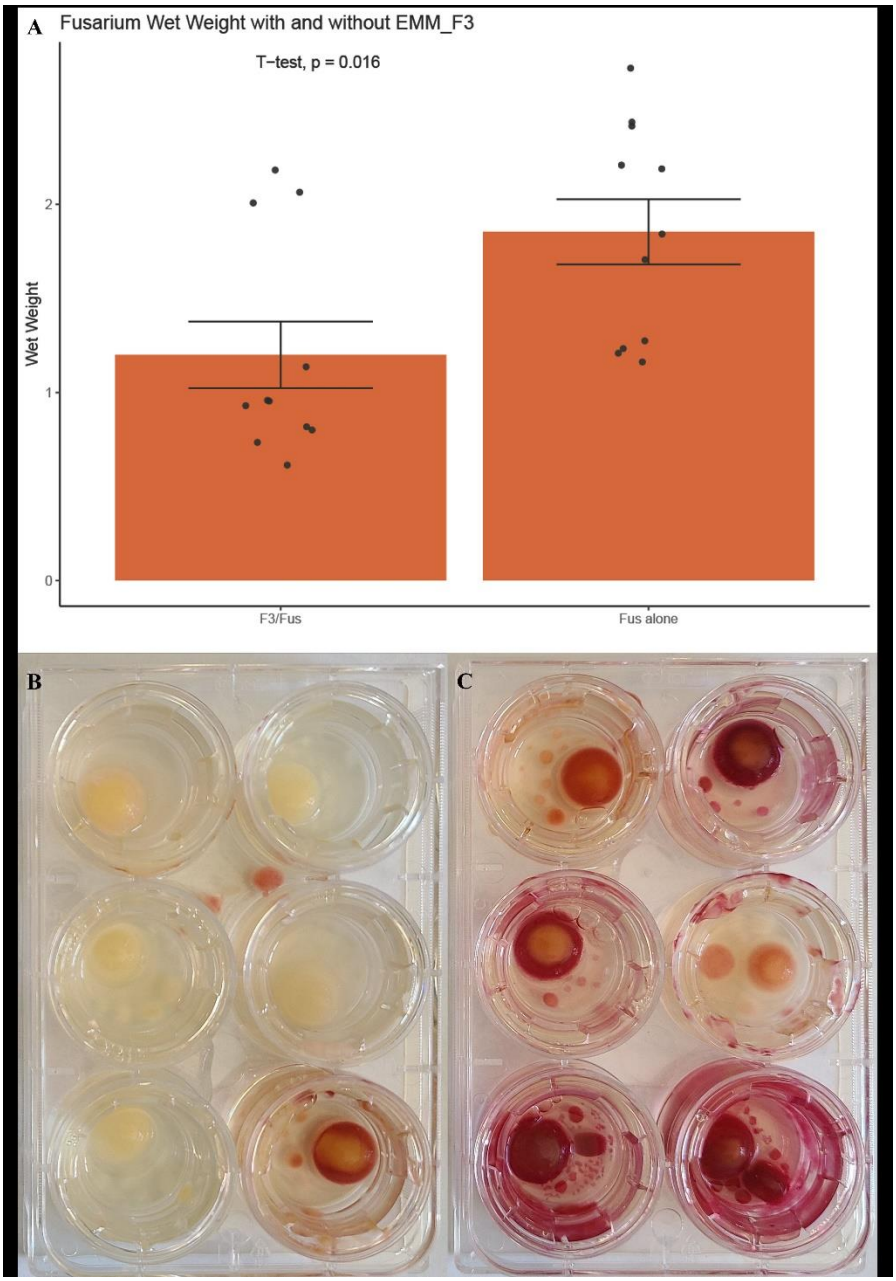

Figure 10. Results of a co-inoculated cell-insert plate experiment to understand EMM_F3's effect on *Fusarium graminearum* isolate PH-1. PH-1 wet weight was taken one week after co-inoculation. Cell-insert plates were inoculated with EMM_F3 on the bottom and a plug of PH-1 on top, with a 0.4µm filter separating the two. (A) Wet weight data, indicating inhibition of PH-1. (B) Co-inoculated wells, with little to no phenotypic change of PH-1. (C) Cell-insert plates with PH-1 alone. Phenotypic color change is observed in every well.

Table 10. Potential biosynthetic gene clusters (BGCs) identified by AntiSMASH for EMM_F3. Seven BGCs matched a known cluster to varying degrees, while the remaining 15 were unknown. There were 22 total identified BGCs.

Region	Type	Most Similar Known Cluster	Potential Functions	Similarity	Source
1.1	NRPS-like, fungal-RiPP-like	unknown	na	na	
3.1	NRP-metallophore, NRPS	unknown	na	na	
4.1	NRPS-like	unknown	na	na	
4.2	terpene	clavaric acid	antitumor	100%	Jayasuria et al., 1998
5.1	NRPS-like	unknown	na	na	
6.1	terpene	unknown	na	na	
10.1	NRPS	unknown	na	na	
14.1	NRPS-like	unknown	na	na	
19.1	T1PKS	scytalone/T3HN	melanin biosynthesis	40%	Chen et al., 2021
27.1	terpene	unknown	na	na	
34.1	T1PKS	ankaflavin/monascin/rubropunctatine/monascorubrin	reduce tumor necrosis factor, decrease intracellular ROS formation	12%	Adin et al., 2022
46.1	NRPS	metachelin C/metachelin A/metachelin A-CE/metachelin B/dimerumic acid 11-mannoside/dimerumic acid	siderophores; antioxidant	37%	Krasnoff et al., 2014
57.1	terpene	unknown	na	na	
61.1	T1PKS, NRPS	unknown	na	na	

76.1	NRPS-like	choline	cell membrane maintenance, cell signaling	100%	Zeisel, 2006
91.1	NRPS-like	unknown	na	na	
107.1	NRPS	unknown	na	na	
155.1	RiPP-like	putisolvin	antiadhesive; potential to lyse zoospores	25%	Kuiper et al., 2004; Chauhan et al., 2023
164.1	RiPP-like	unknown	na	na	
186.1	NRPS-like	unknown	na	na	
188.1	arylpolyene	APE Vf	similar to carotenoids, antioxidant	10%	Schoner et al., 2016; Dong et al., 2024
287.1	NRPS-like	unknown	na	na	

Table 11. A list of the repeat-masked genomes taken from the Joint Genome Institute used for comparative genomics with EMM_F3. Species, isolate, and lifestyle are provided.

Species	Accession Number	funannotate ID	Lifestyle	Lifestyle Source
Aaosphaeria arxii CBS 175.79	PRJNA234399	*Aaosphaeria arxii*	saprobe	Haridas et al., 2020
Alternaria alternata MPI-PUGE-AT-0064	MPI-PUGE-AT-0064	*Alternaria alternata*	pathogen	Haridas et al., 2020
Aureobasidium pullulans NBB 7.2.1	NBB 7.2.1	*Aureobasidium pullulans*	pathogen/saprobe	Haridas et al., 2020
Botryosphaeria dothidea		*Botryosphaeria dothidea*	pathogen	Haridas et al., 2020
Cercospora zeae-maydis SCOH1-5	SCOH1-5	*Cercospora zeae-maydis*	pathogen	Haridas et al., 2020
Cladosporium fulvum		*Fulvia fulva*	pathogen	de Wit et al., 2012

Cochliobolus heterostrophus C4	C4	*Bipolaris maydis*	pathogen	Haridas et al., 2020
Colletotrichum sublineola TX430BB	TX430BB	*Colletotrichum sublineola*	pathogen	Baroncelli et al., 2014
Cryomyces minteri CCFEE 5187	CBS 116302	*Cryomyces minteri*	saprobe	Selbmann et al., 2015
Delphinella strobiligena CBS 735.71	CBS 735.71	*Delphinella strobiligena*	pathogen/saprobe	Haridas et al., 2020
Dothidotthia symphoricarpi CBS 119687	CBS 119687	*Dothidotthia symphoricarpi*	pathogen	Haridas et al., 2020
Elsinoe ampelina CECT 20119	CECT 20119	*Elsinoe ampelina*	pathogen	Haridas et al., 2020
Macrophomina phaseolina MPI-SDFR-AT-0080	MPI-SDFR-AT-0080	*Macrophomina phaseolina*	pathogen	Haridas et al., 2020
Pyricularia oryzae 70-13	70-13	*Pyricularia oryzae*	pathogen	Dean et al., 2005
Mycosphaerella eumusae CBS 114824	CBS 114824	*Pseudocercospora eumusae*	pathogen	Haridas et al., 2020
Myriangium duriaei CBS 260.36	CBS 260.36	*Myriangium duriaei*	pathogen/saprobe	Haridas et al., 2020
Phyllosticta capitalensis CBS 128856	CBS 128856	*Phyllosticta capitalensis*	endophyte	Guarnaccia et al., 2019
Phyllosticta citricarpa CBS 127454	CBS 127454	*Phyllosticta citricarpa*	pathogen	Guarnaccia et al., 2019
Rhizodiscina lignyota CBS 133067	CBS 133067	*Rhizodiscina lignyota*	saprobe	Haridas et al., 2020
Stagonospora nodorum SN15	SN15	*Parastagonospora nodorum*	pathogen	Haridas et al., 2020
Viridothelium virens	PRJNA519654	*Viridothelium virens*	symbiotroph/saprobe	Haridas et al., 2020
Venturia effusa		*Venturia effusa*	pathogen	Winter et al., 2020
Venturia inequalis		*Venturia inequalis*	pathogen	Haridas et al., 2020
Zymoseptoria tritici IP0323	IP0323	*Zymoseptoria tritici*	pathogen	Haridas et al., 2020

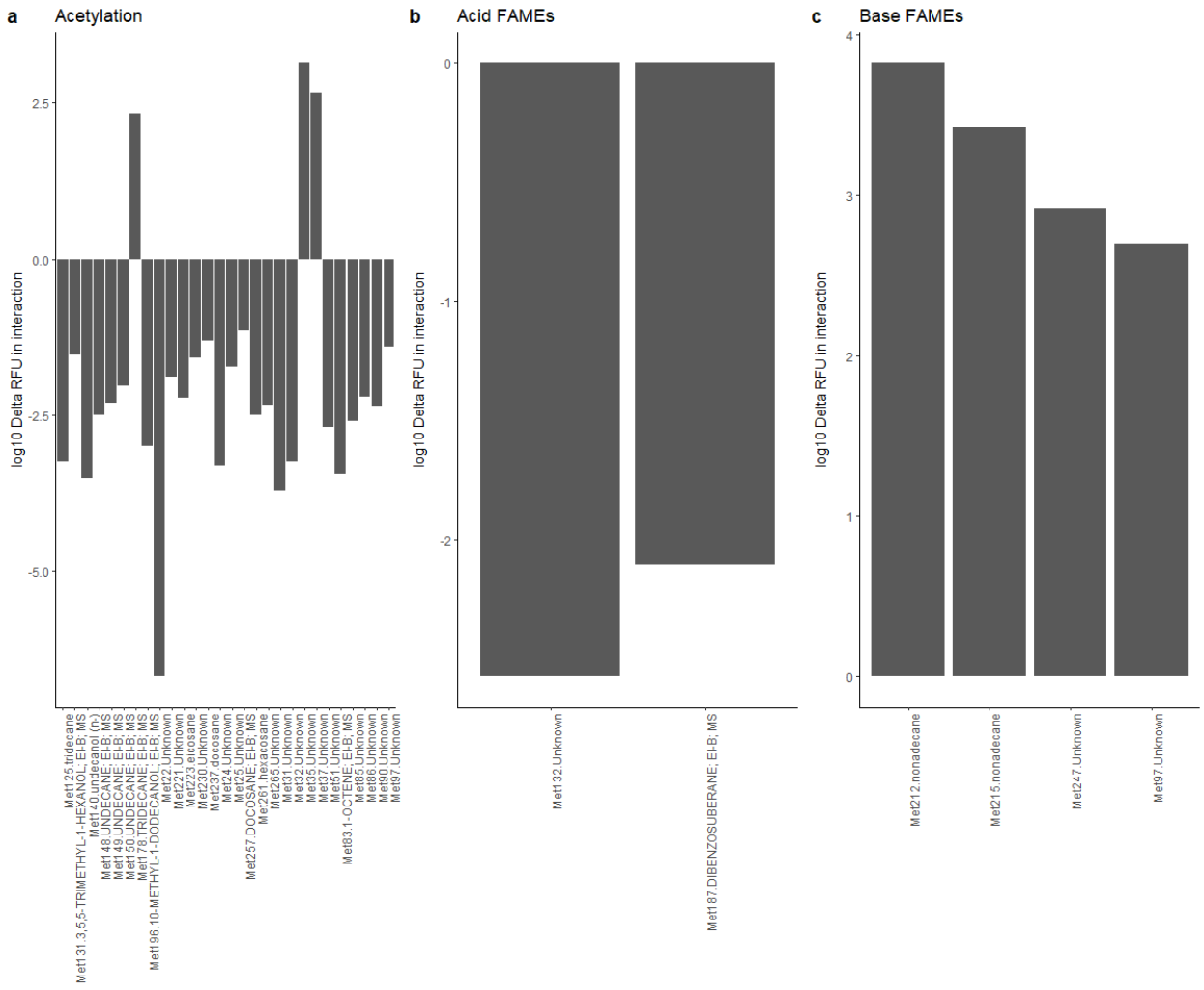

Figure 11. Initial gas chromatography-mass spectrometry (GC-MS) analysis of metabolites unique to EMM_F3, from an EMM_F3/PH-1 co-inoculation extracted at five days post-inoculation. Acid and Base Fatty Acid Methyl Esters (FAMEs) and acetylation extractions were performed. Results indicate that acetylation extractions provided the most diverse results. Values less than zero decreased in EMM_F3 only samples compared to the interaction, and positive values indicate metabolites that are present in a higher amount when taken from EMM_F3 alone. Acetylation extraction provided the most metabolites unique to EMM_F3, with three showing positive values: Met78 (identified as tridecane), Met35 (of unknown identity), and Met37 (of unknown identity). The acid FAMEs extraction did not provide EMM_F3 metabolites that were notably increased when in EMM_F3 alone compared to EMM_F3 in an interacting state. The base FAMEs extraction provided four EMM_F3 metabolites that were increased when compared to EMM_F3 when in an interacting state. Two metabolites, Met212 and Met215, were identified as nonadecane, and the remaining two metabolites, Met247 and Met97, were of unknown identity.

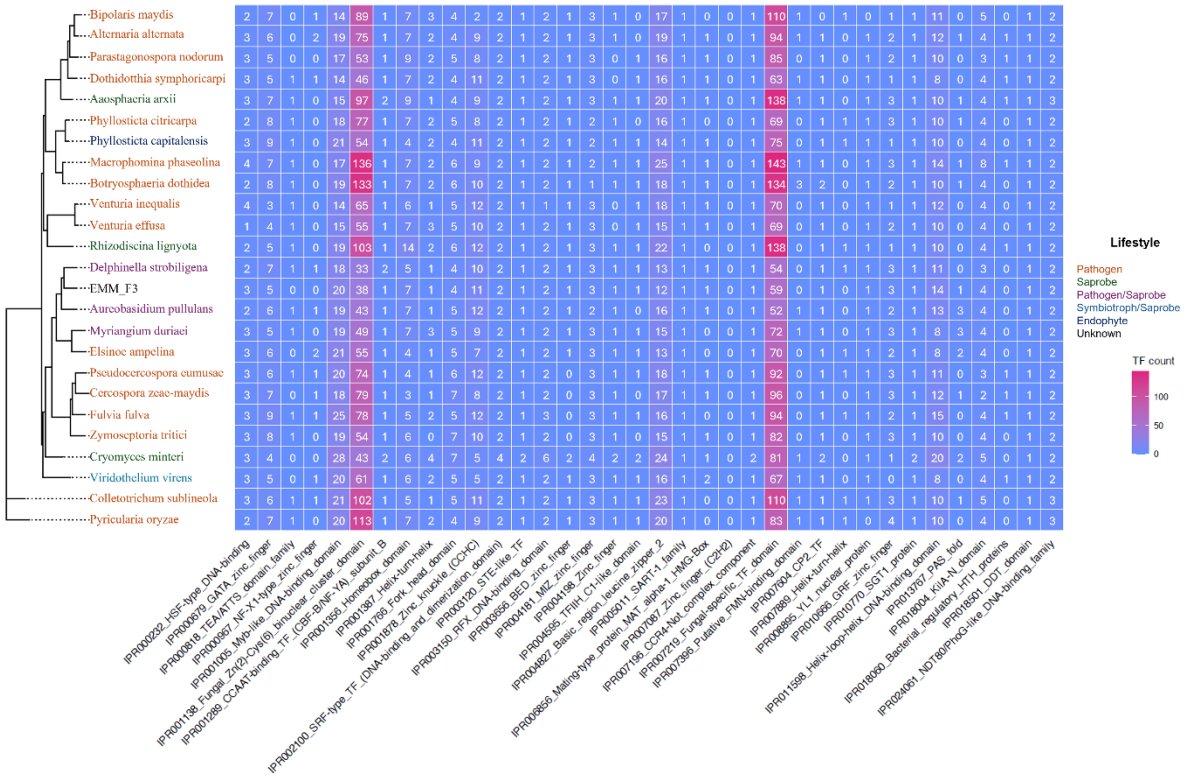

Figure 12. Comparative genomics display of transcription factors and the phylogenetic tree. Both figure sections were generated with data provided as output by the funannotate software. Lifestyles are highlighted in orange (pathogen), green (saprobe), or purple (pathogen/saprobe), blue (symbiotroph/saprobe), dark blue (endophyte), and black (unknown). Lifestyles were taken from Table 10.

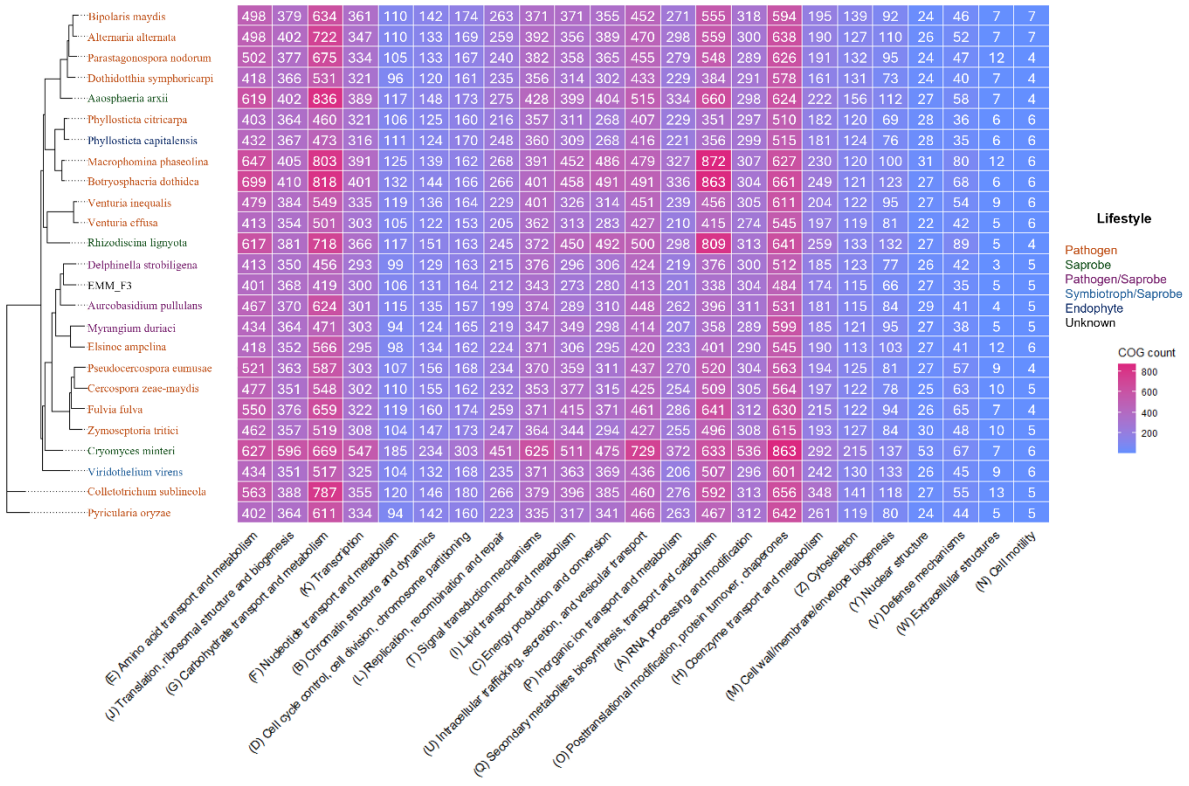

Figure 13. Comparative genomics display of Clusters of Orthologous Genes (COGs) and the phylogenetic tree. Both figure sections were generated with data provided as output by the funannotate software. Lifestyles are highlighted in orange (pathogen), green (saprobe), or purple (pathogen/saprobe), blue (symbiotroph/saprobe), dark blue (endophyte), and black (unknown). Lifestyles were taken from Table 10. The highest counts were carbohydrate transport and metabolism, secondary metabolite biosynthesis, transport and catabolism, posttranslational modification, protein turnover, and chaperones. EMM_F3 does not display excess counts of any gene.

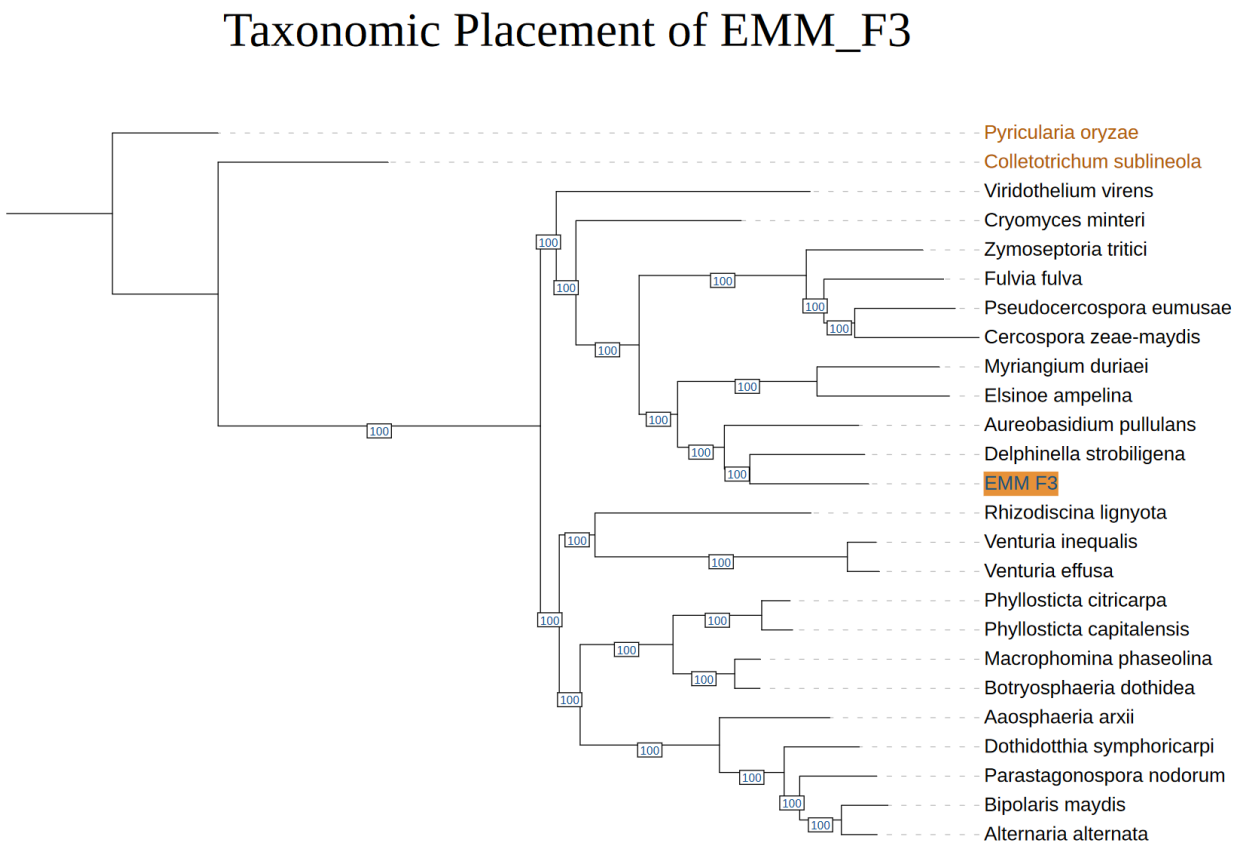

Figure 14. Maximum likelihood tree generated using IQ-TREE through the 'compare' function of the funannotate program based on 500 single copy orthologous genes. Outgroups are from the Sordariomycetes class and are displayed in orange text. EMM_F3 is highlighted in orange. Bootstrap values are displayed in blue and are based on 100 iterations. Figure was edited using iTOL v6 (Letunic & Bork, 2024).

4. CHAPTER FOUR

Conclusions and Impacts

Conclusions

Fungicides are an environmental disturbance that has the potential to impact agricultural ecosystems in various ways despite the necessity to produce viable crop yield. By studying fungicidal effects on the pecan phyllosphere, important knowledge of shifting fungal diversity has been elucidated for a perennial crop with high disease pressure, which may inform future research in similar crop systems. A specific aspect of this is alteration of phyllosphere yeast populations, which are ecologically relevant despite the fact that there is still a plethora of research to be performed on these organisms. By profiling the pecan phyllosphere community under both heavy disease and fungicidal pressure, and classifying a novel Dothideomycete yeast, questions surrounding these topics are being explored in order to inform future research.

Pecan orchards may be sprayed with over 10 fungicide applications a season in order to maintain proper yield, and we studied potential shifts in the fungal phyllosphere with and without the presence of fungicides. We found that fungicides significantly shift fungal community structure, though this effect is not always significant each year. This data is important because other crop systems may be differentially affected, and seasonal variation may play a role in how these effects are displayed. We also found that phyllosphere yeast taxa are differentially abundant in fungicide-treated samples that were significantly different from non-fungicide-treated groups, indicating that these yeasts play an important role in stabilizing disturbed communities and should be studied further.

Due to positive effects of phyllosphere yeasts on fungicide-treated communities, we found it scientifically relevant to study an environmental yeast species isolated from *Magnolia*

grandiflora, known for its hosting of diverse fungal taxa. One yeast stood out from the rest that were tested, EMM_F3. This yeast was chosen for stark phenotypic change, metabolite production, and pathogen suppression, which all encourage the exploration of phylogenetically related yeast for similar properties. After taxonomic placement, it was determined that EMM_F3 matched to the Dothideales clade and was a sister taxon to pine pathogen *Delphinella strobiligena*. This data indicates that EMM_F3 may be a novel pine pathogen itself or could just be a generalist yeast that can thrive in different phyllosphere environments. Preliminary research performed on this yeast informs future researchers in terms of methods used to describe novel yeast taxa and encourages continued classification of novel environmental samples that could provide beneficial effects to the community.

Impacts

Data from Chapter 2 are helpful in recognizing effects of fungicide applications and potential loss of species due to the disturbance caused. In contrast, these data provide hopeful evidence that phyllosphere yeast taxa can assume beneficial roles in stabilizing communities disrupted by these necessary fungicide applications. These data have been presented at the national American Phytopathological Society in 2023, and at the Auburn University College of Agriculture graduate research poster showcase twice (in 2022 and 2023). This chapter is in the process of being drafted and submitted to the Phytobiomes journal.

Data from Chapter 3 build upon conclusions from Chapter 2, highlighting a novel Dothideomycete yeast and its phenotypic, metabolic, and taxonomic properties that can inform researchers of lifestyle and other benefits the yeast may have on its local community. These data have been presented at Auburn University's first Plants, Insects, and Microbes Symposium, and

the chapter is in the process of being drafted and submitted to the Microbiology Spectrum journal.

List of Intended Publications

Refereed publications

1. Anticipated journal: Phytobiomes

   Severance, B. M., Noel, Z. A., 2024. Diversity and effects of fungicides on the pecan phyllosphere microbiome. *Phytobiomes*.

2. Anticipated journal: Microbiology Spectrum

   Severance, B. M., Luchs, L. C., Noel, Z. A., 2024. Describing fungal interactions, metabolism, and taxonomically placing a novel Dothideomycete yeast. *Microbiology Spectrum*.

3. Aided in sequence processing for Elizabeth's fungal data. Details to be determined.

Presentations

1. **Severance, B. M.**, Noel, Z. A., 2023. A tough nut to crack: Fungicides and non-target effects to the pecan phyllosphere microbiome. American Phytopathological Society 2023 National Meeting. ***Poster Presentation***
2. **Severance, B. M.**, Noel, Z. A., 2022. Non-target impacts of routine fungicide applications to the pecan phyllosphere microbiome and interactions with *Venturia effusa*. 2022 Auburn College of Agriculture Graduate Research Poster Showcase. ***Poster Presentation***
3. Severance, B. M., Noel, Z. A., 2023. A tough nut to crack: Fungicides and non-target effects to the pecan phyllosphere microbiome. 2023 Auburn College of Agriculture Graduate Research Poster Showcase. ***Poster Presentation***

4. **Severance, B. M.**, Luchs, L. C., Noel, Z. A., 2024. Fungal interactions, metabolism, and phylogenomic placement of a novel phyllosphere yeast. Auburn University Plants, Insects, and Microbes Symposium. ***Poster Presentation***
5. Moen, F. S., Olofintila, O. E., Alam, J., **Severance, B.**, Noel, Z. A., Goodwin, D. C., Liles, M. A., 2023. Capacity of diverse *Bacillus* species to control both oomycete and fungal pathogens. Southeastern Branch of the American Society for Microbiology 2023 Annual Meeting. ***Poster Presentation***
6. Moen, F. S., Olofintila, O. E., Alam, J., **Severance, B.**, Noel, Z. A., Goodwin, D. C., Liles, M. A., 2024. Capacity of diverse *Bacillus* species to control both oomycete and fungal pathogens. American Society for Microbiology 2024 National Meeting. ***Poster Presentation***

5. References

Chapter 1.

Beckerman, J., et al. (2009). "A 33-year Evaluation of Resistance and Pathogenicity in the Apple Scab-crabapples Pathosystem." Hortscience **44**(3): 599-608.

Bock, C. H., et al. (2014). "Genetic Diversity and Population Structure of Fusicladium effusum on Pecan in the United States." Plant Disease **98**(7): 916-923.

Cadez, N., et al. (2010). "The effect of fungicides on yeast communities associated with grape berries." Fems Yeast Research **10**(5): 619-630.

Charlton, N. D., et al. (2019). First description of the sexual stage of Venturia effusa, causal agent of pecan scab, bioRxiv.

Chen, X., et al. (2021). "Bacterial communities in the plant phyllosphere harbour distinct responders to a broad-spectrum pesticide." Sci Total Environ **751**: 141799.

Conner, P. J. (2002). "A detached leaf technique for studying race-specific resistance to Cladosporium caryigenum in pecan." Journal of the American Society for Horticultural Science **127**(5): 781-785.

Demaree, J. B. (1924). "Pecan scab with special reference to sources of the early spring infections." Journal of Agricultural Research **28**: 0321-0330.

Dickinson, C. H. and B. Wallace (1976). "Effects of late applications of foliar fungicides on activity of micro-organisms on winter wheat flag leaves." Transactions of the British Mycological Society **67**(1): 103-112.

Freimoser, F. M., et al. (2019). "Biocontrol yeasts: mechanisms and applications." World Journal of Microbiology & Biotechnology **35**(10).

Glasby, T. M. and A. J. Underwood (1996). "Sampling to differentiate between pulse and press perturbations." Environmental Monitoring and Assessment **42**(3): 241-252.

Hilbig, J., et al. (2018). "Aqueous extract from pecan nut [Carya illinoinensis (Wangenh) C. Koch] shell show activity against breast cancer cell line MCF-7 and Ehrlich ascites tumor in Balb-C mice." J Ethnopharmacol **211**: 256-266.

Huet, S., et al. (2023). "Experimental community coalescence sheds light on microbial interactions in soil and restores impaired functions." Microbiome **11**(1): 42.

Karlsson, I., et al. (2014). "Fungicide effects on fungal community composition in the wheat phyllosphere." PLOS ONE **9**(11): e111786.

Knief, C., et al. (2010). "Competitiveness of Diverse Methylobacterium Strains in the Phyllosphere of Arabidopsis thaliana and Identification of Representative Models, Including M. extorquens PA1." Microbial Ecology **60**(2): 440-452.

Knorr, K., et al. (2019). "Fungicides have complex effects on the wheat phyllosphere mycobiome." PLOS ONE **14**(3): e0213176.

Lindow, S. E. and M. T. Brandl (2003). "Microbiology of the phyllosphere." Appl Environ Microbiol 69(4): 1875-1883.

Lloyd, A. W., et al. (2021). "Effect of Fungicide Application on Lowbush Blueberries Soil Microbiome." Microorganisms **9**(7): 1366.

Noel, Z. A., et al. (2022). "Non-target impacts of fungicide disturbance on phyllosphere yeasts in conventional and no-till management." ISME Commun **2**(1): 1-10.

Redford, A. J. and N. Fierer (2009). "Bacterial succession on the leaf surface: a novel system for studying successional dynamics." Microbial Ecology **58**(1): 189-198.

Shade, A. (2023). "Microbiome rescue: directing resilience of environmental microbial communities." Curr Opin Microbiol **72**: 102263.

USDA, N. (2021). "Pecan Production."

Winter, D. J., et al. (2020). "Chromosome-Level Reference Genome of Venturia effusa, Causative Agent of Pecan Scab." Molecular Plant-Microbe Interactions **33**(2): 149-152.

Zhang, D. P., et al. (2012). "Cloning, characterization, expression and antifungal activity of an alkaline serine protease of Aureobasidium pullulans PL5 involved in the biological control of postharvest pathogens." International Journal of Food Microbiology 153(3): 453-464.

Chapter 2.

Bowsher, A. W., et al. (2021). "Seasonal Dynamics of Core Fungi in the Switchgrass Phyllosphere, and Co-Occurrence with Leaf Bacteria." Phytobiomes Journal 5(1): 60-68.

Brockhurst, M. A., et al. (2010). "Ecological drivers of the evolution of public-goods cooperation in bacteria." Ecology 91(2): 334-340.

Charlton, N. D., et al. (2019). First description of the sexual stage of Venturia effusa, causal agent of pecan scab, bioRxiv.

CropScience, B. (2019). "Absolute Maxx Fungicide." from https://www.cropscience.bayer.us/d/absolute-maxx-fungicide#phcontent_7_divAccordion.

CropScience, B. (2021). "Stratego YLD." from https://www.greenbook.net/bayer-cropscience/stratego-yld.

Davis, N. M., et al. (2018). "Simple statistical identification and removal of contaminant sequences in marker-gene and metagenomics data." Microbiome 6.

Demaree, J. B. (1924). "Pecan scab with special reference to sources of the early spring infections." Journal of Agricultural Research 28: 0321-0330.

Edgar, R. C. (2010). "Search and clustering orders of magnitude faster than BLAST." Bioinformatics 26(19): 2460-2461.

FRAC (2024). "Search Fungicides to find FRAC Recommendations." from https://www.frac.info/fungicide-resistance-management/by-fungicide-common-name.

Gdanetz, K., et al. (2021). "Influence of Plant Host and Organ, Management Strategy, and Spore Traits on Microbiome Composition." Phytobiomes Journal 5(2): 202-219.

Glenn, D. M., et al. (2015). "Effect of pest management system on 'Empire' apple leaf phyllosphere populations." Scientia Horticulturae 183: 58-65.

Hilbig, J., et al. (2018). "Aqueous extract from pecan nut [Carya illinoinensis (Wangenh) C. Koch] shell show activity against breast cancer cell line MCF-7 and Ehrlich ascites tumor in Balb-C mice." J Ethnopharmacol 211: 256-266.

Knief, C., et al. (2010). "Competitiveness of Diverse Methylobacterium Strains in the Phyllosphere of Arabidopsis thaliana and Identification of Representative Models, Including M. extorquens PA1." Microbial Ecology 60(2): 440-452.

Latin, R. (2021). CHAPTER 2: Modes of Action of Fungicides. A Practical Guide to Turfgrass Fungicides, Second Edition, The American Phytopathological Society: 39-63.

LifeScience, A. (2017). Elast 400 Flowable Fungicide.

Lloyd, A. W., et al. (2021). "Effect of Fungicide Application on Lowbush Blueberries Soil Microbiome." Microorganisms 9(7): 1366.

Longley, R., et al. (2020). "Crop Management Impacts the Soybean (Glycine max) Microbiome." Front Microbiol 11: 1116.

Love, M. I., et al. (2014). "Moderated estimation of fold change and dispersion for RNA-seq data with DESeq2." Genome Biology 15(12).

Lundberg, D. S., et al. (2013). "Practical innovations for high-throughput amplicon sequencing." Nature Methods 10(10): 999-+.

Martin, M. (2011). "Cutadapt removes adapter sequences from high-throughput sequencing reads." EMBnet.journal 17: 10-12.

McMurdie, P. J. and S. Holmes (2013). "phyloseq: An R Package for Reproducible Interactive Analysis and Graphics of Microbiome Census Data." PLOS ONE 8(4).

Noel, Z. A., et al. (2022). "Non-target impacts of fungicide disturbance on phyllosphere yeasts in conventional and no-till management." ISME Commun 2(1): 1-10.

Nufarm (2018). "Phostrol Fungicide." from https://nufarm.com/uscrop/product/phostrol/.

Oksanen J, S. G., Blanchet F, Kindt R, Legendre P, Minchin P, O'Hara R, Solymos P, Stevens M, Szoecs E, Wagner H, Barbour M, Bedward M, Bolker B, Borcard D, Carvalho G, Chirico M, De Caceres M, Durand S, Evangelista H, FitzJohn R, Friendly M, Furneaux B, Hannigan G, Hill M, Lahti L, McGlinn D, Ouellette M, Ribeiro Cunha E, Smith T, Stier A, Ter Braak C, Weedon J (2024). "vegan: Community Ecology Package."

Palmer, J. M., et al. (2018). "Non-biological synthetic spike-in controls and the AMPtk software pipeline improve mycobiome data." PeerJ 6: e4925.

Paulson, J. N. P., M.; Bravo, H.C. (2023). "metagenomeSeq: Statistical analysis for sparse high-throughput sequencing." from https://cbcb.umd.edu/software/metagenomeSeq.

Perazzolli, M., et al. (2014). "Resilience of the Natural Phyllosphere Microbiota of the Grapevine to Chemical and Biological Pesticides." Applied and Environmental Microbiology 80(12): 3585-3596.

Peschel, S., et al. (2021). "NetCoMi: network construction and comparison for microbiome data in R." Briefings in Bioinformatics 22(4).

Redford, A. J. and N. Fierer (2009). "Bacterial succession on the leaf surface: a novel system for studying successional dynamics." Microbial Ecology 58(1): 189-198.

Rognes, T., et al. (2016). "VSEARCH: a versatile open source tool for metagenomics." PeerJ 4.

Schaeffer, R. N., et al. (2017). "Consequences of a nectar yeast for pollinator preference and performance." Functional Ecology **31**(3): 613-621.

Station, A. A. E. (2020). "East-Central Region Alabama Research Units." from https://aaes.auburn.edu/outlying-units/east-central-region/#ev-smith-research-center.

Sun, P. F., et al. (2014). "Indole-3-Acetic Acid-Producing Yeasts in the Phyllosphere of the Carnivorous Plant Drosera indica L." PLOS ONE **9**(12).

United Phosphorus, I. (2010). Supertin 4L.

USDA, N. (2021). "Pecan Production."

Weiss, S., et al. (2017). "Normalization and microbial differential abundance strategies depend upon data characteristics." Microbiome **5**.

Wickham, H. (2009). "ggplot2: Elegant Graphics for Data Analysis." Ggplot2: Elegant Graphics for Data Analysis: 1-212.

Winter, D. J., et al. (2020). "Chromosome-Level Reference Genome of Venturia effusa, Causative Agent of Pecan Scab." Molecular Plant-Microbe Interactions 33(2): 149-152.

Yoon, G., et al. (2019). "Microbial Networks in SPRING - Semi-parametric Rank-Based Correlation and Partial Correlation Estimation for Quantitative Microbiome Data." Frontiers in Genetics 10.

Chapter 3.

Adin, S. N., et al. (2023). "Monascin and ankaflavin-Biosynthesis from Monascus purpureus, production methods, pharmacological properties: A review." Biotechnology and Applied Biochemistry 70(1): 137-147.

Agler, M. T., et al. (2016). "Microbial Hub Taxa Link Host and Abiotic Factors to Plant Microbiome Variation." PLOS Biology 14(1).

Andrews, J. H. and R. F. Harris (2000). "The Ecology and Biogeography of Microorganisms on Plant Surfaces." Annu Rev Phytopathol 38: 145-180.

Andrews, J. H. (1992). “The Fungal Community: its organization and role in the ecosystem.” New York: Marcel Dekker; Chapter 7, Fungal life-history strategies; p. 119–145.

Astashyn, A., et al. (2024). "Rapid and sensitive detection of genome contamination at scale with FCS-GX." Genome Biology 25(1).

Baker, G. B., et al. (1994). "Derivatization with Acetic-Anhydride - Applications to the Analysis of Biogenic-Amines and Psychiatric Drugs by Gas-Chromatography and Mass-Spectrometry." Journal of Pharmacological and Toxicological Methods 31(3): 141-148.

Bankevich, A., et al. (2012). "SPAdes: A New Genome Assembly Algorithm and Its Applications to Single-Cell Sequencing." Journal of Computational Biology 19(5): 455-477.

Baroncelli, R., et al. (2014). "Draft Genome Sequence of Colletotrichum sublineola, a Destructive Pathogen of Cultivated Sorghum." Genome Announcements 2(3).

Blin, K., et al. (2023). "antiSMASH 7.0: new and improved predictions for detection, regulation, chemical structures and visualisation." Nucleic Acids Research 51(W1): W46-W50.

Blum, M. S., et al. (1982). "Biochemistry of Termite Defenses - Coptotermes, Rhinotermes and Cornitermes Species." Comparative Biochemistry and Physiology B-Biochemistry & Molecular Biology **71**(4): 731-733.

Cantalapiedra, C. P., et al. (2021). "eggNOG-mapper v2: Functional Annotation, Orthology Assignments, and Domain Prediction at the Metagenomic Scale." Molecular Biology and Evolution 38(12): 5825-5829.

Chen, X., et al. (2021). "Compartmentalization of Melanin Biosynthetic Enzymes Contributes to Self-Defense against Intermediate Compound Scytalone in Botrytis cinerea." Mbio 12(2).

Chettri, P., et al. (2012). "The veA gene of the pine needle pathogen Dothistroma septosporum regulates sporulation and secondary metabolism." Fungal Genetics and Biology 49(2): 141-151.

de Jager, E. S., et al. (2001). "Microbial ecology of the mango phylloplane." Microbial Ecology 42(2): 201-207.

de Wit, P. J. G. M., et al. (2012). "The Genomes of the Fungal Plant Pathogens Cladosporium fulvum and Dothistroma septosporum Reveal Adaptation to Different Hosts and Lifestyles But Also Signatures of Common Ancestry." Plos Genetics 8(11).

Dean, R. A., et al. (2005). "The genome sequence of the rice blast fungus Magnaporthe grisea." Nature 434(7036): 980-986.

Dvorska, J. E., et al. (2001). "Effect of the mycotoxin aurofusarin on the antioxidant composition and fatty acid profile of quail eggs." British Poultry Science 42(5): 643-649.

Frith, M. C. (2011). "A new repeat-masking method enables specific detection of homologous sequences." Nucleic Acids Research **39**(4).

Gao, P., et al. (2012). "Isolation and identification of C-19 fatty acids with anti-tumor activity from the spores of Ganoderma lucidum (reishi mushroom)." Fitoterapia **83**(3): 490-499.

Gdanetz, K. and F. Trail (2017). "The Wheat Microbiome Under Four Management Strategies, and Potential for Endophytes in Disease Protection." Phytobiomes Journal 1(3): 158-168.

Gostincar, C., et al. (2014). "Genome sequencing of four Aureobasidium pullulans varieties: biotechnological potential, stress tolerance, and description of new species." Bmc Genomics 15.

Gouka, L., et al. (2022). "Ecology and functional potential of phyllosphere yeasts." Trends Plant Sci 27(11): 1109-1123.

Guarnaccia, V., et al. (2019). "Phyllosticta citricarpa and sister species of global importance to Citrus." Molecular Plant Pathology 20(12): 1619-1635.

Gurevich, A., et al. (2013). "QUAST: quality assessment tool for genome assemblies." Bioinformatics 29(8): 1072-1075.

Haridas, S., et al. (2020). "101 Dothideomycetes genomes: A test case for predicting lifestyles and emergence of pathogens." Studies in Mycology 96(1): 141-153.

Hatta, R., et al. (2002). "A conditionally dispensable chromosome controls host-specific pathogenicity in the fungal plant pathogen." Genetics 161(1): 59-70.

Ichihara, K. and Y. Fukubayashi (2010). "Preparation of fatty acid methyl esters for gas-liquid chromatography." Journal of Lipid Research 51(3): 635-640.

Inácio, J., et al. (2002). "Estimation and diversity of phylloplane mycobiota on selected plants in a Mediterranean-type ecosystem in Portugal." Microbial Ecology 44(4): 344-353.

Jayasuriya, H., et al. (1998). "Clavaric acid:: A triterpenoid inhibitor of farnesyl-protein transferase from Clavariadelphus truncatus." Journal of Natural Products 61(12): 1568-1570.

Jones, P., et al. (2014). "InterProScan 5: genome-scale protein function classification." Bioinformatics 30(9): 1236-1240.

Kim, J. E., et al. (2006). "GIP2, a putative transcription factor that regulates the aurofusarin biosynthetic gene cluster in Gibberella zeae." Applied and Environmental Microbiology 72(2): 1645-1652.

Knief, C., et al. (2010). "Competitiveness of Diverse Methylobacterium Strains in the Phyllosphere of Arabidopsis thaliana and Identification of Representative Models, Including M. extorquens PA1." Microbial Ecology 60(2): 440-452.

Krall, B. S., et al. (1999). "Chemical defense in the stink bug Cosmopepla bimaculata." Journal of Chemical Ecology 25(11): 2477-2494.

Krasnoff, S. B., et al. (2014). "Metachelins, Mannosylated and N-Oxidized Coprogen-Type Siderophores from Metarhizium robertsii." Journal of Natural Products 77(7): 1685-1692.

Kuiper, I., et al. (2004). "Characterization of two Pseudomonas putida lipopeptide biosurfactants, putisolvin I and II, which inhibit biofilm formation and break down existing biofilms." Molecular Microbiology 51(1): 97-113.

Kunz, S. (2004). "Development of "Blossom-Protect" - a yeast preparation for the reduction of blossom infections by fire blight."

Letunic, I. and P. Bork (2024). "Interactive Tree of Life (iTOL) v6: recent updates to the phylogenetic tree display and annotation tool." Nucleic Acids Research.

Li, A. H., et al. (2020). "Diversity and phylogeny of basidiomycetous yeasts from plant leaves and soil: Proposal of two new orders, three new families, eight new genera and one hundred and seven new species." Studies in Mycology 96: 17-140.

Li, H. (2018). "Minimap2: pairwise alignment for nucleotide sequences." Bioinformatics **34**(18): 3094-3100.

Lindow, S. E. and M. T. Brandl (2003). "Microbiology of the phyllosphere." Appl Environ Microbiol 69(4): 1875-1883.

Lücking, R. and D. L. Hawksworth (2018). "Formal description of sequence-based voucherless Fungi: promises and pitfalls, and how to resolve them." Ima Fungus 9(1): 143-166.

Maignien, L., et al. (2014). "Ecological Succession and Stochastic Variation in the Assembly of Arabidopsis thaliana Phyllosphere Communities." Mbio 5(1).

Manni, M., et al. (2021). "BUSCO Update: Novel and Streamlined Workflows along with Broader and Deeper Phylogenetic Coverage for Scoring of Eukaryotic, Prokaryotic, and Viral Genomes." Molecular Biology and Evolution 38(10): 4647-4654.

Miguel, M. G., et al. (2013). "Propolis volatiles characterisation from acaricide-treated and -untreated beehives maintained at Algarve (Portugal)." Natural Product Research **27**(8): 743-749.

Minh, B. Q., et al. (2020). "IQ-TREE 2: New Models and Efficient Methods for Phylogenetic Inference in the Genomic Era (vol 37, pg 1530, 2020)." Molecular Biology and Evolution **37**(8): 2461-2461.

Mojarrab, M., et al. (2013). "Chemical composition and general toxicity of essential oils extracted from the aerial parts of Artemisia armeniaca Lam. and A. incana (L.) Druce growing in Iran." Research in Pharmaceutical Sciences **8**(1): 65-69.

Mukherjee, A., et al. (2013). "Alkanes in Flower Surface Waxes of Momordica cochinchinensis Influence Attraction to Aulacophora foveicollis Lucas (Coleoptera: Chrysomelidae)." Neotropical Entomology **42**(4): 366-371.Ohm, R. A., et al. (2012). "Diverse Lifestyles and Strategies of Plant Pathogenesis Encoded in the Genomes of Eighteen Dothideomycetes Fungi." Plos Pathogens 8(12).

Palmer, J. (2017). "Funannotate: Fungal genome annotation scripts."

Parafati, L., et al. (2015). "Biocontrol ability and action mechanism of food-isolated yeast strains against Botrytis cinerea causing post-harvest bunch rot of table grape." Food Microbiology 47: 85-92.

Rodriguez, R. J., et al. (2009). "Fungal endophytes: diversity and functional roles." New Phytologist 182(2): 314-330.

Schoch, C. L., et al. (2009). "A class-wide phylogenetic assessment of Dothideomycetes." Studies in Mycology(64): 1-15.

Schöner, T. A., et al. (2016). "Aryl Polyenes, a Highly Abundant Class of Bacterial Natural Products, Are Functionally Related to Antioxidative Carotenoids." Chembiochem 17(3): 247-253.

Selbmann, L., et al. (2015). "Rock black fungi: excellence in the extremes, from the Antarctic to space." Current Genetics 61(3): 335-345.

Sondergaard, T. E., et al. (2016). "Fast Screening of Antibacterial Compounds from Fusaria." Toxins 8(12).

Todd, J. W. (1989). "Ecology and Behavior of Nezara viridula." Annual Review of Entomology 34: 273-292.

Tsugawa, H., et al. (2015). "MS-DIAL: data-independent MS/MS deconvolution for comprehensive metabolome analysis." Nature Methods 12(6): 523-+.

Tzeng, T. H., et al. (1992). "A Restriction-Fragment-Length-Polymorphism Map and Electrophoretic Karyotype of the Fungal Maize Pathogen Cochliobolus heterostrophus." Genetics 130(1): 81-96.

Vorholt, J. A. (2012). "Microbial life in the phyllosphere." Nature Reviews Microbiology 10(12): 828-840.

Wanasinghe, D. N., et al. (2020). "Taxonomic novelties in Magnolia-associated pleosporalean fungi in the Kunming Botanical Gardens (Yunnan, China)." PLOS ONE 15(7).

Weiss, A. M., G.; Kunz, S. (2006). "Development of "Boni-Protect" - a yeast preparation for use in the control of postharvest diseases of apples." Fördergemeinschaft Ökologischer Obstbau e.V. (FÖKO), pp. 113-117.

Wijayawardene, N. N., et al. (2017). "Notes for genera: Ascomycota." Fungal Diversity 86(1): 1-594.

Winter, D. J., et al. (2020). "Chromosome-Level Reference Genome of Venturia effusa, Causative Agent of Pecan Scab." Molecular Plant-Microbe Interactions 33(2): 149-152.

Zeisel, S. H. (2006). "Choline: Critical role during fetal development and dietary requirements in adults." Annual Review of Nutrition 26: 229-250.

Zeng, Q., et al. (2023). "Aureobasidium pullulans from the Fire Blight Biocontrol Product, Blossom Protect, Induces Host Resistance in Apple Flowers." Phytopathology 113(7): 1192-1201.

Zhang, D. P., et al. (2012). "Cloning, characterization, expression and antifungal activity of an alkaline serine protease of Aureobasidium pullulans PL5 involved in the biological

control of postharvest pathogens." International Journal of Food Microbiology 153(3): 453-464.